to compare the after-drug-challenge continuous ECG phenotypes between *SCN5A* mutation–negative and –positive Brugada syndrome patients. Correlations between quantitative phenotypes before and after sodium channel blockade are expressed as Pearson correlation coefficients (*r*). For comparison of the proportion of male subjects, Fisher's exact test was used.

The effect of haplotype pairs on the continuous ECG phenotypes was tested in the Brugada syndrome patients and control subjects separately by ANOVA with adjustment for age and gender. The 9 *SCN5A* mutation–positive Brugada syndrome patients were treated as a separate category (7 HapA/HapA homozygotes, 2 HapA/HapB heterozygotes, pooled). The 2 individuals with the rare HapC variant (1 patient from each group) were excluded from analyses. In all analyses, the proportion of variance attributable to the haplotype pair (R^2) was calculated and corrected for the effects of age and gender.

Differences in reporter gene expression activity between HapA and HapB were examined for statistical significance with Student's *t* test. Throughout, values of $P < 0.05$ were interpreted as being significant. All statistical analyses were done with SAS software (version 9, SAS Institute).

Multiple Testing

When a Bonferroni correction for the 24 statistical models is used to compare the continuous ECG phenotypes, the significance level for the overall probability values is 0.002. Similarly, the Bonferroni-corrected significance levels for the pairwise comparisons between 3 and 4 groups is 0.017 and 0.008, respectively.

Results

Haplotypes

The 6 polymorphisms were in near-complete linkage disequilibrium, with only 2 (similar) discordant haplotypes (of 364; <1%), each occurring in 1 subject from each population. We designated HapA as containing all common alleles and HapB as containing all minor alleles (Figure 1). The discordant haplotype was designated HapC. The estimated frequencies of HapA, HapB, and HapC were 0.755, 0.240, and 0.005 in the control subjects and 0.782, 0.211, and 0.007 in the *SCN5A* mutation–negative Brugada syndrome patients, respectively. Haplotype distributions were in Hardy-Weinberg equilibrium ($P > 0.05$) in both populations. No significant difference in haplotype frequencies was observed between the Brugada syndrome group and the control subjects. The haplotypes were absent in white and black samples.

Functional Analysis

In cardiomyocytes, reporter activity of HapB was markedly reduced, by 62%, compared with HapA: 5.5 ± 0.4 (mean$\pm$SE) versus 14.5 ± 2.8 (normalized activity units; n=9 each; $P = 0.006$; Figure 2). A similar trend was seen in the noncardiac cells: 2.7 ± 0.3 versus 3.6 ± 0.3 (n=13 each; $P = 0.04$; Figure 2).

Phenotypic Characteristics of the Control and Brugada Syndrome Patient Populations

The decreased reporter activity for HapB suggested that individuals carrying this promoter haplotype would display ECG-detectable conduction slowing. Accordingly, the relationships between genotype and ECG intervals were evaluated in the control and Brugada syndrome populations.

ECG data are shown in Table 1. As expected, Brugada syndrome patients had significantly longer conduction intervals (PR_{II}, QRS_{V1}, QRS_{V6}) and greater ST-segment elevation
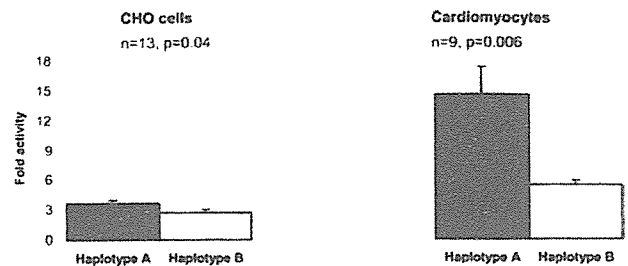

Figure 2. Reporter activity of *SCN5A* promoter haplotypes A and B. Firefly luciferase expression levels, which report the activities of the inserted *SCN5A* sequence, were divided by coexpressed Renilla luciferase activities and expressed as relative luciferase units.[7] Data are presented as mean$\pm$SE (vs empty vector). CHO indicates Chinese hamster ovary.

(ST_J, ST_{80}) compared with control subjects. Heart rate was not significantly different between the 2 populations. In addition, we found differences between *SCN5A* mutation–positive and *SCN5A* mutation–negative Brugada syndrome patients similar to those previously reported[10]: Mutation-positive subjects had significantly longer baseline PR and QRS intervals and longer RR intervals. Data on the subset of Brugada syndrome patients who underwent drug challenge are presented in Table 2. For all ECG parameters investigated, highly significant ($P < 0.0001$) correlations were present between measures before and after drug challenge (Table 2). As previously reported, *SCN5A* mutation–positive patients displayed longer PR and QRS intervals after challenge with sodium channel blockers compared with *SCN5A* mutation–negative patients.[10]

Haplotype Pair Effects

PR and QRS durations were significantly longer in HapB individuals in both study populations (Brugada syndrome and control subjects: $P \le 0.002$ for PR_{II}; $P < 0.0001$ for QRS_{V1} and QRS_{V6}; Figure 3). In the control population, PR_{II}, QRS_{V1}, and QRS_{V6} intervals showed a gene-dose effect, being longest in HapB homozygotes, intermediate in HapA/HapB heterozygotes, and shortest in HapA homozygotes. A similar pattern was observed in the *SCN5A* mutation–negative Brugada syndrome patient group. As discussed earlier, these analyses excluded data in the 2 individuals with HapC. PR_{II}, QRS_{V1}, and QRS_{V6} means ($\pm$SD) per haplotype group for the 2 populations are listed in the Data Supplement Table II. Both the overall and pairwise probability values were highly statistically significant even after correction for multiple testing.

The amount of variance (R^2) in PR and QRS intervals explained by the haplotype pair after correction for age and gender is shown in Table 3. As can be seen, a significant proportion of variance in PR and QRS intervals, both at baseline (both groups) and after drug challenge (Brugada syndrome group), was attributable to the haplotype. No significant association was found between haplotype and RR, ST_J, and ST_{80} in either population (data not shown).

Drug Challenge and Haplotype

The haplotype pairs were also highly associated with conduction intervals (PR_{II}, QRS_{V1}, QRS_{V6}) after sodium channel

TABLE 1. Baseline ECG Characteristics of the Control and Brugada Syndrome Patient Populations

| | Control Subjects | Brugada Syndrome Patients | | | Pairwise Comparison P | |
		SCN5A⁻ᵛᵉ	SCN5A⁺ᵛᵉ	Overall P	SCN5A⁻ᵛᵉ vs SCN5A⁺ᵛᵉ	SCN5A⁻ᵛᵉ vs Control Subjects
n	102	71	9			
Male, n (%)	67 (66)	67 (94)	9 (100)	<0.0001	1.000	<0.0001
Age, y	40.0±14.2	46.5±16.3	51.1±8.4	0.005	0.376	0.005
RR, ms	925.3±130.0	913.7±134.3	1055.6±154.2	0.012	0.003*	0.572
PR$_{II}$, ms	162.3±21.8	180.4±20.4	238.9±26.7	<0.0001*	<0.0001*	<0.0001*
QRS$_{V1}$, ms	93.8±11.8	104.9±19.3	142.2±19.1	<0.0001*	<0.0001*	<0.0001*
QRS$_{V6}$, ms	87.4±12.4	100.2±19.1	139.4±21.6	<0.0001*	<0.0001*	<0.0001*
ST$_J$, mV	0.10±0.05	0.30±0.14	0.34±0.18	<0.0001*	0.249	<0.0001*
ST$_{80}$, mV	0.18±0.10	0.25±0.12	0.24±0.13	0.001*	0.778	0.001*

Values are given as mean±SD.
*Below the Bonferroni-corrected overall or pairwise significance levels (see Multiple Testing).

blockade in 44 *SCN5A* mutation–negative Brugada syndrome patients who underwent drug challenge (for PR$_{II}$, QRS$_{V1}$, QRS$_{V6}$, P<0.0001; Figure 3). PR$_{II}$, QRS$_{V1}$, and QRS$_{V6}$ means (±SD) per haplotype group are listed in the Data Supplement Table II. Here also, overall and pairwise probability values were highly statistically significant even after correction for multiple testing.

In addition, the extent of QRS widening (ΔQRS) after drug challenge was genotype dependent, and a gene-dose effect was also observed (ΔQRS$_{V6}$: HapB/HapB=30 ms [mean± SD]; HapA/HapB=24.2±7.9; HapA/HapA=17.8±7.2; P=0.002; Figure 4). A similar trend was seen for extent of PR widening (ΔPR) after drug challenge (ΔPR$_{II}$: HapB/HapB=40 ms; HapA/HapB=33.8±13.2; HapA/HapA=28.6±8.3; P=0.05).

Discussion

We demonstrate that a set of 6 *SCN5A* promoter polymorphisms found in Asian subjects are in near-complete linkage disequilibrium, have a significant impact on sodium

channel expression in vitro, account for a large proportion of variance in ECG conduction parameters in 2 independent Japanese populations, and represent pharmacogenetic markers predicting variable drug response.

Twin studies have identified strong genetic effects for ECG parameters, including PR and QRS durations.[11–14] Indeed, associations have been reported between ECG parameters and single coding region nonsynonymous (amino acid–changing) SNPs in ion channel genes.[15,16] However, common functional variants in regulatory regions that strongly modulate basal ECG intervals have not previously been identified; 1 preliminary report has suggested an association between a potassium channel promoter polymorphism and QRS axis in women only.[17] Only recently has the concept of tightly linked polymorphisms (constituting a haplotype block) been applied to understanding variability in cardiac electrophysiology. In 1 study, a small degree of variance (<1%) in QT interval in a central European population could be attributed to single SNPs and haplotype blocks in 4 potassium channel genes.[18]

TABLE 2. Clinical Characteristics of the Brugada Syndrome Patients After Sodium Channel Blocker Challenge

	SCN5A⁻ᵛᵉ	SCN5A⁺ᵛᵉ	P	r, Before and After Sodium Channel Blockade
n	44	5		
Male, n (%)	42 (95)	5 (100)	1.000	
Age, y	46.3±14.8	52.0±5.4	0.397	
aRR, ms	892.3±113.1	956.0±99.4	0.234	0.94
aPR$_{II}$, ms	209.6±25.1	278.0±35.6	<0.0001*	0.95
aQRS$_{V1}$, ms	124.1±16.1	166.0±17.8	<0.0001*	0.92
aQRS$_{V6}$, ms	119.2±17.1	166.0±17.8	<0.0001*	0.92
aST$_J$, mV	0.51±0.21	0.78±0.25	0.013	0.84
aST$_{80}$, mV	0.41±0.17	0.70±0.31	0.109	0.63

Values are given as mean±SD. Pearson correlation coefficients (r) observed between measures before and after sodium channel blocker challenge (P<0.0001). Mean baseline ECG parameters for the 44 *SCN5A*⁻ᵛᵉ and 5 *SCN5A*⁺ᵛᵉ patients (not shown) were very similar to those for the total patient group given in Table 1.
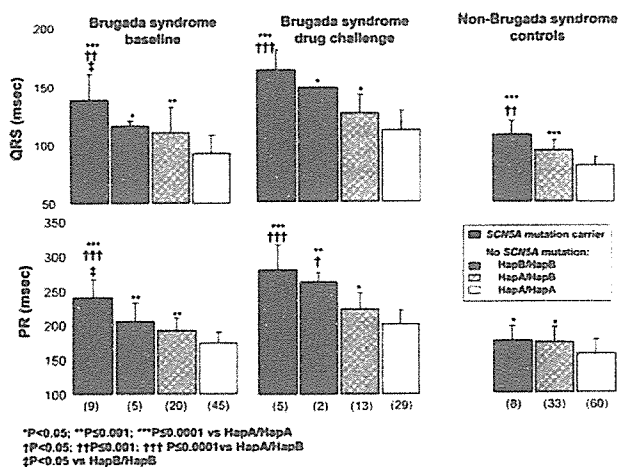*Below the Bonferroni-corrected overall significance levels (see Multiple Testing).

*P<0.05; **P≤0.001; ***P≤0.0001 vs HapA/HapA
†P<0.05; ††P≤0.001; ††† P≤0.0001vs HapA/HapB
‡P<0.05 vs HapB/HapB

Figure 3. *SCN5A* promoter haplotype effects on durations of QRS$_{V6}$ and PR$_{II}$ in Brugada syndrome patients at baseline and after challenge with sodium channel blocking agents and in non–Brugada syndrome control subjects. Patient numbers are indicated in parentheses. Genotype effects on QRS$_{V1}$ were similar to those on QRS$_{V6}$ because of a high correlation between these 2 parameters (Pearson's coefficient, $r=0.96$). Data are presented as mean±SD. For Bonferroni-corrected significance levels for pairwise comparisons, refer to the Multiple Testing section in Patients and Methods.

In contrast, the *SCN5A* promoter haplotype we report here explained a remarkable proportion of variance in conduction parameters in the Japanese subjects studied (Table 3). Such associations could arise because the haplotypes studied are, in turn, in linkage disequilibrium with other functionally important variants in regulatory or other regions of the gene. However, in this case, the in vitro functional studies indicate that the effect is attributable to a variant within the haplotype block; at this point, the specific variant mediating this effect has not been identified.

A principal determinant of cardiac conduction in atrial and ventricular muscle is the sodium current; sodium channel blockers prolong PR and QRS durations, an effect also seen with loss of function mutations in *SCN5A*.[3] Critical degrees of conduction slowing represent a final common pathway to VF,[19] so dissection of the genetic determinants of cardiac conduction in the general population is a key step to understanding variable susceptibility to common arrhythmias resulting from conduction slowing, as in myocardial ischemia

TABLE 3. Variance Explained by the Haplotype Pair

	R^2, %		
	Control Subjects	Brugada Syndrome Baseline	Brugada Syndrome Drug Challenge
PR$_{II}$	12.2	28.4	33.0
QRS$_{V1}$	47.6	26.4	33.0
QRS$_{V6}$	48.5	24.9	36.2

or heart failure.[19] Thus, the data we present here implicate the *SCN5A* promoter variant HapB, which slowed conduction in normal subjects and exacerbated conduction slowing in those with Brugada syndrome, as a candidate modulator of variability in risk of SCD. Importantly, imposition of further depression of sodium channel function by administration of sodium channel blocking drugs further exacerbated conduction slowing in a gene-dose-dependent fashion. Studies in large numbers of subjects at risk for SCD are required to further establish the role of this and other regulatory region polymorphisms in modulating that risk.

Differences in disease penetrance and expression have been widely reported in the cardiac sodium and other channelopathies.[20-23] Relatives carrying an *SCN5A* mutation identical to that of the proband may be clinically unaffected,[20] and family members may display different phenotypes, eg, Brugada syndrome or conduction disease.[23] Genetic variants like the one presented here are obvious candidate modulators of this variability in phenotypic expression. Interindividual variability also has been noted in response to pharmacological challenge with sodium channel blockers in Brugada syndrome patients.[20,24] In some patients, even some carrying an *SCN5A* mutation, drug challenge fails to unmask a Brugada syndrome ECG. The significantly greater increases in PR and QRS durations with sodium channel blockade in HapB carriers thus identify variability in expression of the drug target, the sodium channel, as a key mediator of this variable drug effect. It is thus possible that other sodium channel blocker response phenotypes such as the increased mortality with sodium channel blockers in the CAST[2] was determined by variable sodium channel expression. DNA samples from that important clinical trial were not archived, so this question will remain unanswered. More generally, the data
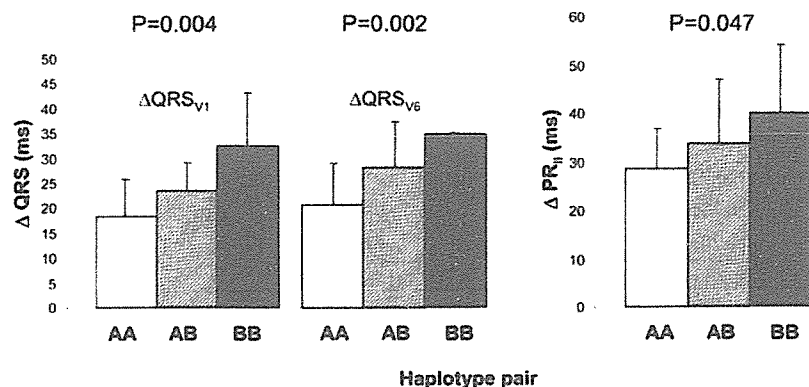

Haplotype pair

Figure 4. *SCN5A* promoter haplotype effects on extent of QRS (ΔQRS$_{V1}$ and ΔQRS$_{V6}$) and PR (ΔPR$_{II}$) widening after sodium channel blockade. AA, n=29; AB, n=13; BB, n=2. Data are presented as mean±SD. The Bonferroni-corrected significance level is 0.002.

indicate that sodium channel function is additively suppressed by drug challenge, Brugada syndrome mutations, and the HapB regulatory variant. Although a strong reduction in reporter gene activity was observed for HapB compared with HapA in vitro, the extent to which this reduction translates proportionately into reduced sodium channel density in vivo is unknown.

Brugada syndrome is endemic in Asia, where the disorder is also known as sudden unexplained nocturnal death syndrome[25]; in fact, the incidence is higher in Asia than in the United States and Europe.[26] Because HapB is common in Asians and absent in whites and has a large negative impact on cardiac conduction, a long-recognized feature of Brugada syndrome,[27] it may logically contribute to differences in Brugada syndrome incidence as a function of ethnicity. In this study, PR and QRS durations in individuals matched for haplotype were consistently longer in the Brugada syndrome group compared with control subjects; thus, the greatest conduction slowing was in those subjects with Brugada syndrome and the HapB/HapB genotype. Indeed, control HapB/HapB subjects had longer QRS durations than did those with manifest Brugada syndrome and the commoner HapA/HapA genotype. Thus, although the minor allele is quite common, it alone may give rise to one part of the spectrum of loss of sodium channel function that constitutes the Brugada syndrome. However, data at this stage do not indicate that HapB per se leads to Brugada syndrome.

More generally, the data fit nicely the concept that individuals vary in their ability to maintain sodium channel function to protect against the arrhythmia-prone substrate and identify HapB as a variant that contributes to such variable "antifibrillatory reserve."[10,28]

Disclosures

Drs Shimizu and Miyamato are applying for a Japanese domestic patent based on this work. The other authors report no conflicts.

References

1. De Vreede-Swagemakers JJ, Gorgels AP, Dubois-Arbouw WI, van Ree JW, Daemen MJAP, Houben LGE, Wellens HJJ. Out-of-hospital cardiac arrest in the 1990's: a population-based study in the Maastricht area on incidence, characteristics and survival. *J Am Coll Cardiol.* 1997;30:1500–1505.
2. Cardiac Arrhythmia Suppression Trial (CAST) Investigators. Preliminary report: effect of encainide and flecainide on mortality in a randomized trial of arrhythmia suppression after myocardial infarction. *N Engl J Med.* 1989;321:406–412.
3. Tan HL, Bezzina CR, Smits JP, Verkerk AO, Wilde AA. Genetic control of sodium channel function. *Cardiovasc Res.* 2003;57:961–973.

4. Bezzina CR, Rook MB, Groenewegen WA, Herfst LJ, van der Wal AC, Lam J, Jongsma HJ, Wilde AAM, Mannens MMAM. Compound heterozygosity for mutations (W156X and R225W) in *SCN5A* associated with severe cardiac conduction disturbances and degenerative changes in the conduction system. *Circ Res.* 2003;92:159–168.
5. Royer A, van Veen TA, Le Bouter S, Marionneau C, Griol-Charhbik V, Léoni AL, Steenman M, van Rijen HVM, Demolombe S, Goddard CA, Ricker C, Escoubet B, Jarry-Guichard T, Colledge WH, Gros D, de Bakker JMT, Grace AA, Escande D, Charpentier F. Mouse model of *SCN5A*-linked hereditary Lenegre's disease: age-related conduction slowing and myocardial fibrosis. *Circulation.* 2005;111:1738–1746.
6. Priori SG, Barhanin J, Hauer RNW, McKenna WJ, Roden DM, Rudy Y, Schwartz K, Schwartz PJ, Towbin JA, Wilde A. Genetic and molecular basis of cardiac arrhythmias: impact on clinical management: Study Group on Molecular Basis of Arrhythmias of the Working Group on Arrhythmias of the European Society of Cardiology. *Eur Heart J.* 1999;20:174–195.
7. Yang P, Kupershmidt S, Roden DM. Cloning and initial characterization of the human cardiac sodium channel (SCN5A) promoter. *Cardiovasc Res.* 2004;61:56–65.
8. Wilde AAM, Antzelevitch C, Borggrefe M, Braugada J, Brugada R, Brugada P, Corrado D, Hauer RNW, Kass RS, Nademanee K, Priori SG, Towbin JA. Proposed diagnostic criteria for the Brugada syndrome: consensus report. *Circulation.* 2002;106:2514–2519.
9. Excoffier L, Slatkin M. Maximum-likelihood estimation of molecular haplotype frequencies in a diploid population. *Mol Biol Evol.* 1995;12:921–927.
10. Smits JPP, Eckardt L, Probst V, Bezzina CR, Schott JJ, Remme CA, Haverkamp W, Breithardt G, Escande DD, Schulze-Bahr E, Le Marec H, Wilde AAM. Genotype-phenotype relationship in Brugada syndrome: electrocardiographic features differentiate SCN5A-related patients from non-SCN5A-related patients. *J Am Coll Cardiol.* 2002;40:350–356.
11. Busjahn A, Knoblauch H, Faulhaber HD, Boeckel T, Rosenthal M, Uhlmann R, Hoeke M, Schuster H, Luft FC. QT interval is linked to 2 long-QT syndrome loci in normal subjects. *Circulation.* 1999;99:3161–3164.
12. Hanson B, Tuna N, Bouchard T, Heston L, Eckert E, Lykken D, Segal N, Rich S. Genetic factors in the electrocardiogram and heart rate of twins reared apart and together. *Am J Cardiol.* 1989;63:606–609.
13. Havlik RJ, Garrison RJ, Fabsitz R, Feinleib M. Variability of heart rate, P-R, QRS and Q-T durations in twins. *J Electrocardiol.* 1980;13:45–48.
14. Moller P, Heiberg A, Berg K. The atrioventricular conduction time: a heritable trait? III: twin studies. *Clin Genet.* 1982;21:181–183.
15. Bezzina CR, Verkerk AO, Busjahn A, Jeron A, Erdmann J, Koopmann TT, Bhuiyan ZA, Wilders R, Mannens MMAM, Tan Hl, Luft FC, Schunkert H, Wilde AAM. A common polymorphism in KCNH2 (HERG) hastens cardiac repolarization. *Cardiovasc Res.* 2003;59:27–36.
16. Splawski I, Timothy KW, Tateyama M, Clancy CE, Malhotra A, Beggs AH, Cappuccio FP, Sagnella GA, Kass RS, Keating MT. Variant of SCN5A sodium channel implicated in risk of cardiac arrhythmia. *Science.* 2002;297:1333–1336.
17. Connor RE, Nguyen T, Palmer AD, Stewart AFR, Pepine CJ, Reichek N, Rogers WJ, McNamara DM, Reis SE, London B. A HERG promoter polymorphism affects QRS axis in women. *Circulation* 2000;102(suppl II):II-261. Abstract.
18. Pfeufer A, Jalilzadeh S, Perz S, Mueller JC, Hinterseer M, Illig T, Akyol M, Huth C, Schöpfer-Wendels A, Kuch B, Steinbeck G, Hoke R, Näbauer M, Wickmann HE, Meitinger T, Kääb S. Common variants in myocardial ion channel genes modify the QT interval in the general population: results from the KORA study. *Circ Res.* 2005;96:693–701.
19. Tomaselli GF, Zipes DP. What causes sudden death in heart failure? *Circ Res.* 2004;95:754–763.
20. Priori SG, Napolitano C, Gasparini M, Pappone C, Della Bella P, Brignole M, Giodano U, Giovannini T, Menozzi C, Bloise R, Crotti L, Terreni L, Schwartz PJ. Clinical and genetic heterogeneity of right bundle branch block and ST-segment elevation syndrome: a prospective evaluation of 52 families. *Circulation.* 2000;102:2509–2515.
21. Priori SG, Napolitano C, Schwartz PJ. Low penetrance in the long-QT syndrome: clinical impact. *Circulation.* 1999;99:529–533.
22. Hong K, Brugada J, Oliva A, Berruezo-Sanchez A, Potenza D, Pollevick GD, Guerchicoff A, Matsuo K, Burashnikov E, Dumaine R, Towbin JA, Nesterenko V, Brugada P, Antzelevitch C, Brugada R. Value of electrocardiographic parameters and ajmaline test in the diagnosis of Brugada syndrome caused by SCN5A mutations. *Circulation.* 2004;110:3023–3027.

23. Kyndt F, Probst V, Potet F, Demolombe S, Chevallier JC, Baró I, Moisan JP, Boisseau P, Schott JJ, Escande D, Le Marec H. Novel SCN5A mutation leading either to isolated cardiac conduction defect or Brugada syndrome in a large French family. *Circulation.* 2001;104: 3081–3086.

24. Wolpert C, Echternach C, Veltmann C, Antzelevitch C, Thomas GP, Spehl S, Streitner F, Kuschyk J, Schimpf R, Haase KK, Borggrefe M. Intravenous drug challenge using flecainide and ajmaline in patients with Brugada syndrome. *Heart Rhythm.* 2005;2:254–260.

25. Vatta M, Dumaine R, Varghese G, Richard TA, Shimizu W, Aihara N, Nademanee K, Brugada R, Brugada J, Veerakul G, Li H, Bowles NE, Brugada P, Antzelevitch A, Towbin JA. Genetic and biophysical basis of sudden unexplained nocturnal death syndrome (SUNDS), a disease allelic to Brugada syndrome. *Hum Mol Genet.* 2002;11:337–345.

26. Meregalli PG, Wilde AA, Tan HL. Pathophysiological mechanisms of Brugada syndrome: depolarization disorder, repolarization disorder, or more? *Cardiovasc Res.* 2005;67:367–378.

27. Brugada P, Brugada J. Right bundle branch block, persistent ST segment elevation and sudden cardiac death: a distinct clinical and electrocardiographic syndrome: a multicenter report. *J Am Coll Cardiol.* 1992;20: 1391–1396.

28. Roden DM. The problem, challenge and opportunity of genetic heterogeneity in monogenic diseases predisposing to sudden death. *J Am Coll Cardiol.* 2002;40:357–359.

CLINICAL PERSPECTIVE

The sodium current determines conduction velocity in the heart, and reducing sodium current predisposes to VF. Sodium channel blockers increased sudden death after MI in CAST, and at least some cases of the Brugada syndrome, in which structurally normal hearts are prone to VF, are due to loss of function mutations in the cardiac sodium channel gene *SCN5A*. Thus, variability in the synthesis of sodium channels could contribute to variable conduction velocity in heart and to VF susceptibility. This study represents an important first step to testing that hypothesis. A set of 6 DNA variants were identified in the *SCN5A* promoter, the region of the gene directing transcriptional activity. The variants are common but only in Asian subjects and are in tight linkage disequilibrium; ie, subjects have either wild-type sequences or all 6 variants, defining a haplotype block called HapB here. HapB sequences not only reduced transcriptional activity in vitro but also predicted slower conduction velocity, assessed by PR and QRS durations, in both Japanese control and Brugada syndrome subjects. The longest QRS durations were in Brugada syndrome patients homozygous for HapB ($\approx$7%) challenged with sodium channel blockers. Indeed, normal subjects homozygous for HapB had longer QRS durations than Brugada syndrome patients homozygous for wild-type sequences. These data support the idea that common *SCN5A* promoter variants modulate conduction velocity and thus susceptibility to VF in response to challenges such as other arrhythmogenic mutations, sodium channel blocking drugs, or acute ischemia. In addition, HapB may contribute to the higher prevalence of Brugada syndrome in Asians.

Genotype-Specific Onset of Arrhythmias in Congenital Long-QT Syndrome
Possible Therapy Implications

Hanno L. Tan, MD, PhD; Abdennasser Bardai, MSc; Wataru Shimizu, MD, PhD; Arthur J. Moss, MD; Eric Schulze-Bahr, MD; Takashi Noda, MD; Arthur A.M. Wilde, MD, PhD

Background—The identification of the molecular-genetic substrate underlying the various forms of the congenital long-QT syndrome (LQTS) has sparked studies into possible genotype–phenotype correlations with the aim of developing genotype-tailored therapy. The onset of torsade de pointes (TdP) may differ among LQTS patients, being pause dependent in some but not all. This disparity may point to different arrhythmia mechanisms and may affect therapy strategies. We studied whether the proportion of pause-dependent TdP onset varies among LQTS genotypes.

Methods and Results—We studied all LQT1 (n=10), LQT2 (n=34), and LQT3 (n=6) patients from 4 centers for whom ECGs of TdP onset were available and analyzed whether pauses preceded TdP onset (first available ECG per patient). Pauses preceded TdP significantly more often in LQT2 (68%) than in LQT1 (0%), and the interval immediately before TdP (pause interval) was significantly longer in LQT2 than in LQT1. The proportion of pause dependence in LQT3 (33%) appeared intermediate, but this group was too small for statistical analysis.

Conclusions—Pause dependence of TdP onset is predominant in LQT2 but absent or rare in LQT1. It is suggested that disparities in pause dependence of TdP onset may reflect different arrhythmia mechanisms. (*Circulation.* 2006;114: 2096-2103.)

Key Words: arrhythmia ■ electrophysiology ■ genetics ■ long-QT syndrome ■ torsade de pointes

The congenital long-QT syndrome (LQTS) is a familial heart disorder that is associated with a prolonged QT interval, T-wave abnormalities, and torsade de pointes (TdP) ventricular tachycardias that may cause syncope and occasionally sudden death. The diagnosis is based on clinical variables, including QT prolongation, a history of syncope, and/or documented TdP episodes.[1] Molecular genetic studies have established that most congenital LQTS forms are caused by mutations in genes that encode cardiac ion channels.[2] Among genotyped patients, mutations in *KCNQ1* (LQT1), *KCNH2* (LQT2), and *SCN5A* (LQT3) are the most prevalent by far.[3] *KCNQ1* and *KCNH2* both encode components of the delayed rectifier potassium current (I_{Ks} and I_{Kr}, respectively), with I_{Kr} being the target of several antiarrhythmic and nonantiarrhythmic drugs with TdP potential.[4] *SCN5A* encodes the cardiac sodium channel.[5]

Clinical Perspective p 2103

The identification of these gene variants has sparked studies into possible genotype–phenotype correlations in LQTS with the aim of refining clinical management and providing genotype-tailored therapy.[6] These studies have revealed that ECG patterns[7] and symptom triggers[8,9] are genotype specific, thus facilitating the establishment of a molecular genetic diagnosis using a candidate-gene approach.[10] Similarly, therapy strategies may be refined because prognosis[11] and the risk of cardiac events[12] are genotype dependent. Moreover, the efficacy of β-blockers, long established as the mainstay of therapy in congenital LQTS,[13] in preventing TdP episodes may be genotype dependent, being higher in LQT1 than in LQT2[14] or LQT3.[9,13,14] This disparity in efficacy may be due to differences in arrhythmia mechanisms. Of note, TdP onset may or may not be pause dependent, ie, associated with pauses that immediately precede the first TdP beat.[15,16] This distinction may reflect different electrophysiological mechanisms and affect the therapeutic efficacy of β-blockers. Identification of those patients who have pause-dependent TdP gains significance because these patients may benefit from ancillary treatment with pacemakers,[17-19] which use algorithms to prevent bradycardias
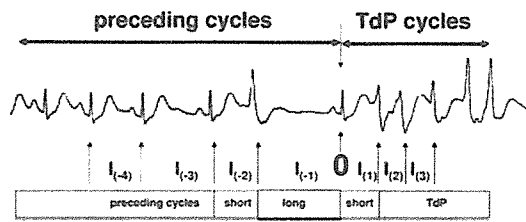
Figure 1. Method of ECG analysis. RR intervals $I_{(-4)}$ through $I_{(3)}$ are numbered with respect to last supraventricular beat (designated 0) before the TdP episode.

and pauses. Accordingly, we studied whether differences exist in pause dependence of TdP onset between LQT1, LQT2, and LQT3.

Methods

Patient Inclusion

We included all LQT1, LQT2, and LQT3 patients from research groups in the Netherlands (n=23), the International LQT Registry in the United States (n=12), Japan (n=9), and Germany (n=6) for whom ECGs of TdP onset were available that contained at least 3 RR intervals directly preceding TdP. Accordingly, we included 10 LQT1 patients from 10 families (7 whites, 3 Asians), 34 LQT2 patients from 30 families (26 whites, 8 Asians), and 6 LQT3 patients from 6 white families. ECGs were obtained from 12-lead ECGs (n=14, 28% of all ECG tracings), telemetry (n=32, 64%), and stored intracardiac electrograms of implantable cardioverter-defibrillators (n=4, 8%). Patients were included only if TdP occurred in the absence of other potential causes, eg, drugs with TdP potential and metabolic imbalances.[20]

ECG Analysis

TdP was defined as a polymorphic ventricular tachycardia of ≥3 beats with a QRS axis that revolved around the baseline (the latter was not required when only intracardiac electrograms of tachycardia were available). In 22 patients, multiple TdP episodes were available. For primary analysis, we studied only 1 episode per patient to avoid overrepresentation of patients for whom an excessive number of TdP episodes were available (in 1 LQT2 patient, 151 episodes during 1 admission were available); moreover, we elected to analyze only the first TdP episode to minimize

the risk that any intervention instituted after the first TdP episode may have modified the mode of onset of subsequent TdP episodes. Being conscious of this latter possible confounder, we also analyzed subsequent TdP episodes in a secondary analysis to obtain an impression about the reproducibility of these findings. The mode of TdP onset was analyzed as shown in Figure 1. RR intervals were numbered with respect to the last supraventricular beat before TdP onset (designated 0). Thus, a short-long-short sequence[15] initiating TdP involves intervals $I_{(-2)}$-$I_{(-1)}$-$I_{(1)}$. The last 3 consecutive RR intervals preceding TdP were measured, along with the TdP cycle length (from the first 3 TdP beats, ie, averaged from $I_{(2)}$ and $I_{(3)}$). In addition, we analyzed the rate of the preceding sinus rhythm. This analysis was thwarted by the facts that bigeminy often preceded TdP and that ECGs were not always recorded for sufficiently long periods surrounding TdP episodes. Thus, analysis of the rate of the sinus rhythm that preceded TdP was possible in only 32 of 50 patients (LQT1, 9; LQT2, 18; LQT3, 5). Sinus beats were analyzed if they occurred within 10 seconds before TdP onset. No generally accepted quantitative criteria to define TdP onset as pause dependent exist. Here, we considered TdP onset to be pause dependent when the duration of $I_{(-1)}$ exceeded that of $I_{(-2)}$ by ≥50% (arbitrary cutoff).

Statistical Analysis

Data are mean±SD. Group comparisons were made with the Fisher exact test (proportions) or the Mann-Whitney test (averages) when appropriate. Statistical significance was defined as $P<0.05$.

The authors had full access to and take full responsibility for the integrity of the data. All authors have read and agree to the manuscript as written.

Results

Patient Characteristics

Demographic variables were not significantly different between the LQTS groups (Tables 1 through 3). There was a marked preponderance of female patients (41 female, 9 male). The proportion of patients taking β-blockers (maximally tolerated doses) was similar among the LQTS groups: LQT1, 4 of 10 (40%); LQT2, 16 of 34 (47%); and LQT3, 1 of 6 (17%).

Pause Dependence of First TdP Episode

ECG analysis is summarized in Tables 1 through 3. When we analyzed the first TdP episode in each patient, we found that

TABLE 1. Demographic and ECG Variables in LQT1

	Age, y	Sex	Mutation	β-Blocker	$I_{(-3)}$, ms	$I_{(-2)}$, ms	$I_{(-1)}$, ms	$I_{(1)}$, ms	$I_{(2)}$, ms	$I_{(3)}$, ms	SR, ms	TdP, ms	Pause-Dependent First TdP	Pause-Dependent TdP, n	Non–Pause-Dependent TdP, n
LQT1 Patients	2	M	G269D	−	520	720	570	470	300	300	NA	300	...	0	1
	7	F	Del GGT (intron)	+	445	430	470	430	250	210	450	230	...	0	1
	8	F	G269S	+	500	480	500	460	270	240	490	255	...	0	1
	9	F	A344V	−	600	530	710	410	270	260	690	265	...	0	1
	11	F	G189R	+	420	420	420	420	270	210	420	240	...	0	3
	12	M	V254M	−	360	380	400	320	240	160	600	200	...	0	1
	15	F	A341V	+	600	630	600	510	360	250	640	305	...	0	2
	18	F	Y315S	−	800	600	680	480	280	230	640	240	...	0	1
	49	F	R259C	−	770	580	740	600	400	340	780	370	...	0	5
	64	F	G569A	−	890	810	810	630	400	280	810	340	...	0	2
Mean	20				591	558	590	473	304	248	613	276			
SD	20				177	138	142	91	60	51	138	52			

SR indicates RR interval of sinus rhythm; NA, not available.

TABLE 2. Demographic and ECG Variables in LQT2

	Age	Sex	Mutation	β-Blocker	$I_{(-3)}$, ms	$I_{(-2)}$, ms	$I_{(-1)}$, ms	$I_{(1)}$, ms	$I_{(2)}$, ms	$I_{(3)}$, ms	SR, ms	TdP, ms	Pause-Dependent First TdP	Pause-Dependent TdP, n	Non–Pause-Dependent TdP, n
LQT2 Patients	1 d	F	G628S	−	740	460	700	520	360	320	560	340	+	1	0
	3 d	F	R1047L	−	600	470	670	400	360	250	490	305	−	0	1
	6 y	M	G628S	+	700	540	1050	630	315	315	NA	315	+	6	0
	7 y	M	Dup 558-600	−	970	580	830	590	350	330	NA	340	−	0	1
	8 y	M	Not released	−	1225	825	825	640	390	360	1250	375	−	2	2
	11 y	F	G628S	+	660	640	740	600	420	360	680	390	−	0	1
	14 y	F	R823W	−	380	580	660	380	300	280	NA	290	−	0	1
	14 y	F	T623I	+	560	330	980	470	310	240	NA	275	+	6	0
	18 y	F	A558P	−	720	720	640	440	320	290	710	305	−	0	1
	19 y	F	R148W+F98S	−	1000	800	1150	600	400	400	1000	400	−	0	1
	20 y	F	E698X	+	410	280	1240	590	320	310	600	315	+	2	1
	21 y	F	P334L	+	600	380	920	520	290	270	NA	280	+	2	3
	21 y	F	F106L	+	750	630	1010	650	470	590	NA	530	+	2	1
	21 y	F	Dup 362bp	−	540	540	1080	410	310	200	870	255	+	1	0
	22 y	F	A614V	−	780	580	960	640	460	380	NA	420	+	1	0
	24 y	F	G785V	+	600	540	1150	590	400	280	735	340	+	2	2
	27 y	F	N633S	+	800	800	1600	700	600	400	NA	500	+	2	0
	28 y	F	R252G	+	570	550	570	400	240	400	580	320	−	0	1
	28 y	F	R534C	−	760	520	960	500	270	370	510	320	+	1	0
	28 y	F	S818L	−	600	400	1200	600	400	320	640	360	+	1	0
	28 y	F	N633S	+	700	240	1160	640	380	320	NA	350	+	1	0
	32 y	F	N996I	−	560	460	620	600	440	300	560	370	−	0	1
	36 y	F	G604S	−	580	300	1200	640	280	320	NA	300	+	25	42
	41 y	M	A558P	+	1140	590	870	630	360	310	1200	335	−	2	2
	41 y	F	M574V	+	400	1350	1010	670	480	410	990	445	−	0	1
	42 y	F	D501N	−	320	320	1260	600	360	340	NA	350	+	18	3
	48 y	F	R582C	+	470	500	1300	680	400	320	NA	360	+	91	0
	59 y	M	W927X	−	750	535	1165	665	335	335	NA	335	+	149	2
	62 y	F	R912fs	−	1360	600	1320	640	360	300	NA	330	+	2	0
	65 y	F	C64Y	+	650	580	1510	610	330	290	615	310	+	1	0
	72 y	M	A558P	+	1350	580	1390	630	420	320	1640	370	+	4	0
	74 y	F	Not released	−	1040	660	1080	640	280	320	1170	300	+	3	0
	79 y	F	F29L	+	660	380	1760	680	420	380	NA	400	+	1	0
	79 y	F	R582C	−	600	600	1220	620	440	280	NA	360	+	3	0
Mean	34 y				729	569	1049	588	374	331	822	353			
SD	22 y				260	201	287	97	72	67	321	59			

SR indicates RR interval of sinus rhythm; Not released, gene variant not released by the molecular-genetic laboratory; and NA, not available.

pause dependence of TdP onset was genotype dependent, being significantly more prevalent in LQT2 (23 of 34, 68%; Figure 2) than in LQT1 (0 of 10, 0%; $P=0.0001$; Figure 3). Accordingly, analysis of average RR intervals revealed that the $I_{(-1)}$ interval (the "long" or "pause" interval) was significantly longer in LQT2 (1044 ± 296 ms; Figure 4) than in LQT1 (590 ± 142 ms; Figure 5) ($P<0.001$). Moreover, the increase in cycle length between the $I_{(-2)}$ and $I_{(-1)}$ intervals was significantly larger in LQT2 than in LQT1 (479 ± 364 versus 32 ± 94 ms; $P<0.001$; Figure 6). TdP cycle length in LQT1

(276 ± 52 ms) was significantly shorter than in LQT2 (353 ± 59 ms; $P=0.001$), but sinus rhythm cycle length was not significantly different between groups (613 ± 138 and 822 ± 321 ms, respectively; $P=0.14$). In LQT3, the prevalence of pause dependence appeared to be intermediate (2 of 6, 33%), as were the duration of the $I_{(-1)}$ intervals (859 ± 279 ms) and the cycle length increase from $I_{(-2)}$ to $I_{(-1)}$ (153 ± 290 ms; Figure 7). Because of the relatively small number of LQT3 patients, we did not conduct statistical comparisons between LQT3 and the 2 other LQT groups.

TABLE 3. Demographic and ECG Variables in LQT3

	Age	Sex	Mutation	β-Blocker	$I_{(-3)}$, ms	$I_{(-2)}$, ms	$I_{(-1)}$, ms	$I_{(1)}$, ms	$I_{(2)}$, ms	$I_{(3)}$, ms	SR, ms	TdP, ms	Pause-Dependent First TdP	Pause-Dependent TdP, n	Non–Pause Dependent TdP, n
LQT3 Patients	1d	F	P1332L	−	1010	1010	1010	875	610	610	990	670	−	0	1
	4y	M	R1623Q	−	440	440	445	295	230	185	440	208	−	0	1
	17y	F	P701L	−	840	865	800	530	440	400	800	420	−	0	1
	20y	F	I176V	−	960	760	760	600	340	260	830	300	−	0	2
	57y	F	I1768V	+	610	590	1180	630	340	310	600	325	+	1	0
	76y	F	I1278N	−	1080	720	1170	700	390	330	NA	360	+	1	0
Mean	29y				795	707	859	548	363	314	732	339			
SD	31y				233	166	279	139	79	83	214	81			

SR indicates RR interval of sinus rhythm; NA, not available.

Influence of Gender and the Use of β-Blockers on First TdP Episode

Pause dependence was not sex dependent because it occurred in similar proportions in male patients (4 of 9, 44%) and female patients (20 of 41, 49%). The proportion of patients with pause-dependent TdP despite the use of β-blockers was lower in LQT1 (0 of 4, 0%) than in LQT2 (12 of 16, 75%; $P=0.01$). Nevertheless, the use of β-blockers did not modify whether pause dependence was present or absent because the proportion of pause dependence among LQT1 and LQT2 patients was similar among those who used β-blockers and those who did not, as follows: LQT1—pause dependence with β-blockers, 0 of 4 (0%), without β-blockers, 0 of 6 (0%); LQT2—pause dependence with β-blockers, 12 of 16 (75%), without β-blockers, 11 of 18 (61%).

Reproducibility of Pause Dependence

To study the reproducibility of pause dependence, we analyzed subsequent TdP episodes in the 22 patients with multiple TdP episodes. Results are summarized in Tables 1 through 3. Four LQT1 patients had multiple TdP episodes (range, 2 to 5); consistent with their first TdP episode, all subsequent TdP episodes were not pause dependent. In LQT2 patients, pause dependence was generally reproducible, as follows: All 17 LQT2 patients with multiple TdP episodes had pause-dependent TdP onset (2 to 91 episodes each). In 8 patients, all subsequent TdP episodes also were

pause dependent. In 5 of the remaining 9 LQT2 patients with multiple episodes, subsequent TdP episodes were generally consistent with the first episode, being mostly pause dependent in 4 patients (3 to 151 episodes) and not pause dependent in 1 patient. However, in 4 LQT2 patients, subsequent TdP episodes were not generally consistent with the first. One LQT3 patient had 2 TdP episodes; both were not pause dependent.

Discussion

We found that pause dependence of TdP onset in congenital LQTS was genotype specific, being predominant in LQT2 but absent in LQT1. In contrast to previous studies,[21] we did not find that the proportion of pause dependence was greater in female than male patients.

Proposed Arrhythmia Mechanisms and Therapy Implications

The disparity in pause dependence of TdP onset between LQT1 and LQT2 may point to different arrhythmia mechanisms. Clinical[22] and experimental[23] studies have provided evidence that pause-dependent TdP is triggered by
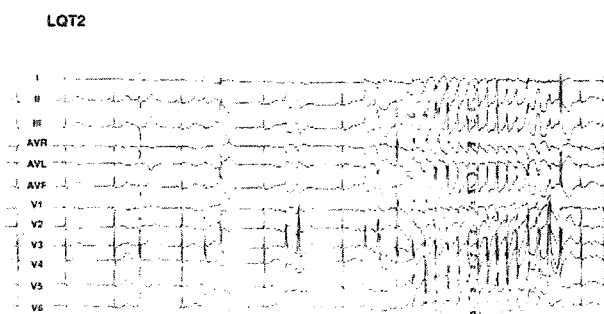
LQT2

Figure 2. Typical example of TdP onset in an LQT2 patient (pause dependent).
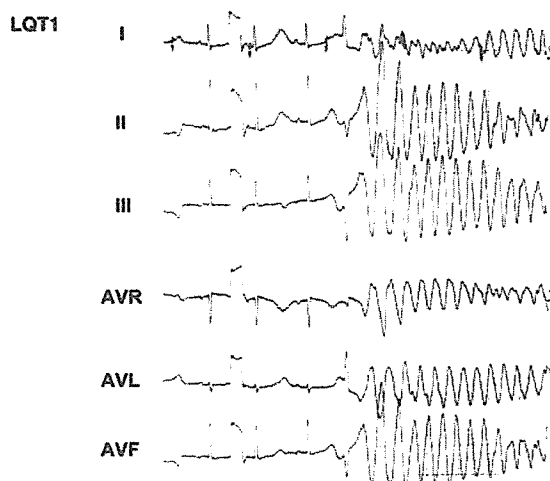
LQT1

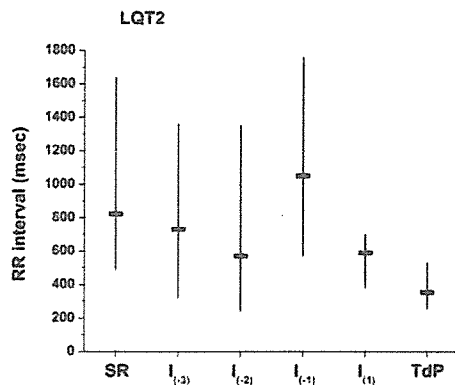**Figure 3.** Typical example of TdP onset in an LQT1 patient (not pause dependent).

Figure 4. RR intervals (shortest-average-longest) surrounding TdP episodes in LQT2 patients. Designation of intervals $I_{(-3)}$ through $I_{(1)}$ as in Figure 1. Note that the ordinate scale is different from that in Figures 5 and 7 to include high values of the longest RR intervals. SR indicates sinus rhythm.
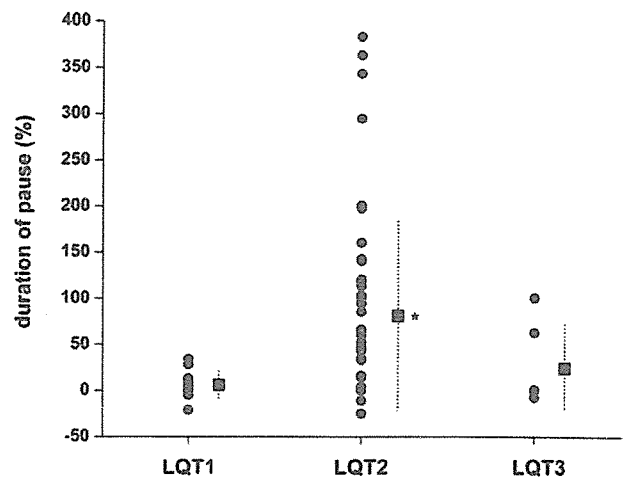
early afterdepolarizations (EADs) carried by L-type Ca^- channels. Numerical analysis has revealed that a pause (after a relatively fast heart rate) leads to enhanced Ca^{2-} release from intracellular Ca^{2+} stores.[24] Subsequently, Ca^{2+}-dependent transmembrane currents (electrogenic Na^+/Ca^{2+} exchanger, I_{Ks}) are altered in such a way as to allow L-type Ca^+ channels to recover more readily from inactivation and to reactivate before repolarization is complete, thus generating EADs. Of note, a critical duration of the pause is required for EADs to occur,[24] comfortably supporting a beneficial role of pause-preventing pacemaker algorithms. At the same time, the absence of pause dependence in LQT1 suggests that EADs are not the predominant mechanism of TdP initiation here. Conversely, the relatively fast heart rate preceding TdP in LQT1 may be compatible with delayed afterdepolarizations (DADs) secondary to intracellular Ca^{2+} overload,[25] although it does not fully exclude EADs.[26] Accordingly, experimental studies have shown that I_{Ks} blockade (LQT1) causes DADs but not EADs.[27] Conversely, experimental I_{Kr} blockade (LQT2) causes EADs, predominantly at slow heart rates.[28] Either way, the proposed involvement of both

Figure 6. Duration of pause expressed as percentage increase in RR interval from $I_{(-2)}$ to $I_{(-1)}$ and calculated as $(I_{(-2)}-I_{(-1)})/I_{(-2)} \times 100$. Shown are individual patients and mean±SD for each LQT group. *$P<0.05$ for LQT1 vs LQT2.

DADs and pause-dependent EADs provides a rationale for the use of β-blockers in that these drugs counteract loading of intracellular Ca^{2+} stores by cAMP-dependent processes, notably Ca^{2+} influx through L-type Ca^+ channels.[29] Ca^{2+} loading as a leitmotiv for TdP was further substantiated by experimental models of LQT2, which revealed the therapeutic efficacy of interventions to reduce intracellular Ca^{2+} loading through other pathways, eg, calmodulin-dependent pathways.[30] Analysis of QT duration (as a measure of action potential duration) would have the potential of providing more mechanistic insights. Increased Ca^{2+} loading, occurring in parallel with QT prolongation, would facilitate DADs and DAD-dependent TdP. Unfortunately, we were unable to investigate a possible relationship between QT duration and pause dependence. In a large proportion of patients, analysis of QT duration was impossible because multiple ventricular premature beats preceded TdP onset and ECGs were not recorded for sufficiently long periods surrounding TdP episodes. Still, other mechanisms also may explain the therapeutic effects of
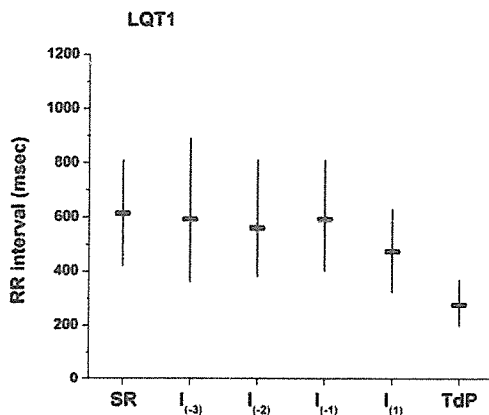

Figure 5. RR intervals surrounding TdP episodes in LQT1 patients. SR indicates sinus rhythm.
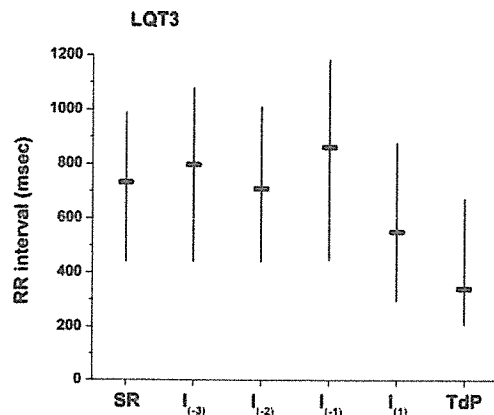

Figure 7. RR intervals surrounding TdP episodes in LQT3 patients. SR indicates sinus rhythm.

β-blockers, in particular, β-adrenergic modulation of I_{K_s}[31] and I_{K_r}.[32–35] Normally, β-adrenergic stimulation increases I_{K_s} and may mediate action potential shortening at fast heart rates. However, when physiological regulation of I_{K_s} by β-adrenergic signaling is disrupted, eg, by mutations in the I_{K_s} complex, action potential duration alternans at fast heart rates may occur, a phenomenon associated with susceptibility to reentrant tachyarrhythmias.[31] β-Adrenergic regulation of I_{K_r} may be more complex (reviewed elsewhere[32]). Some studies showed that acute[33] and chronic[34] β-adrenergic stimulation reduces I_{K_r}. From these studies, β-adrenergic blockade would be expected to increase I_{K_r} and shorten action potential duration, which would explain its beneficial effects. However, other studies[35] showed that β-adrenergic stimulation increases I_{K_r}.

When these proposed electrophysiological mechanisms are considered for genotype-specific therapy, it is predicted that β-blockers alone have great efficacy in preventing non–pause-dependent TdP (LQT1), whereas β-blockers and pacemakers may work in a complementary fashion in pause-dependent TdP (LQT2). These predictions are supported by previous observations that β-blockers are less effective in preventing TdP in LQT2 than in LQT1.[14] Thus, LQT2 patients not only are likely to respond the best to pacemaker therapy but also may require it the most. Still, it must be emphasized that β-blockers remain the cornerstone of congenital LQTS treatment (at least in LQT1 and LQT2) and that pacemaker therapy must be considered an ancillary treatment mode, particularly in LQT2.

Our findings also may provide further rationale for the management of acquired (drug-induced) LQTS. The predominant pause dependence of TdP onset in LQT2 found here corresponds with observations that drug-induced TdP in acquired LQTS is usually pause dependent[20] because these drugs generally block I_{K_r}.[4] Accordingly, (temporary) pacing is also highly effective in acquired LQTS.

Study Limitations

We have defined pause dependence by a clear, yet arbitrary, $\geq 50\%$ increase of $I_{(-1)}$ duration over $I_{(-2)}$ duration. Previous studies have used other arbitrary cutoff values, ie, any increment,[15] a 20-ms increment,[36] or a 40-ms increment[21] over $I_{(-2)}$. To study whether the choice for any particular cutoff value may confound our primary analysis, we also analyzed the proportions of pause-dependent TdP onset in LQT1 and LQT2 when cutoff values other than 50% were used to define "pause dependence" (Figure 8). We found that the proportions of pause-dependent TdP onset remained significantly higher in LQT2 than in LQT1 when cutoff values of 0% ($P=0.04$), 20 ms ($P=0.04$), 40 ms ($P=0.004$), 10% ($P=0.001$), 25% ($P=0.001$), 75% ($P=0.003$), and 100% ($P=0.007$) were used. This analysis provided further support for our conclusion that pause-dependent TdP onset is far more common in LQT2 than in LQT1.

Although LQT1 and LQT2 are equally prevalent (each estimated to account for 40% to 45% of genotyped patients[3]), we found that ECG documentation of TdP onset
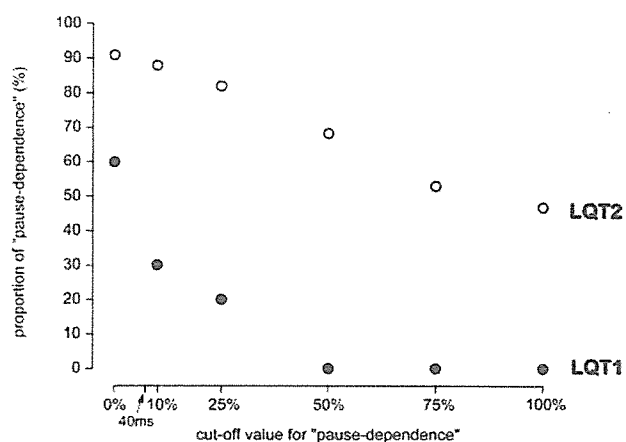

Figure 8. Proportion of pause-dependent TdP onset in LQT1 (●) and LQT2 (○) at various definitions of pause dependence.

was far more prevalent in LQT2. The reasons are a matter of speculation. For instance, it may relate to the fact that TdP in LQT1 occurs mostly during exercise.[8,9] Thus, TdP is less likely to recur and be documented during hospital admission. In contrast, TdP in LQT2 may be triggered by anxiety, which may continue during admission.[37] Also, because β-blocker treatment is less effective in LQT2, TdP may still be readily observed during admission. Whatever the cause, the difficulty in obtaining ECG documentation of TdP onset in LQT1 may explain why the reported proportion of pause-dependent TdP onset in congenital LQTS is as high as 74% in some studies,[21] although it should be only a little over 50%, given that TdP is rarely pause dependent in LQT1 and that LQT1 constitutes almost 50% of congenital LQTS. This discrepancy may be caused by underrepresentation of LQT1 patients because these patients are less easily included in such analyses. How the reported proportion of pause dependence could be confounded by overrepresentation or underrepresentation of LQT3 patients is unclear because it is unresolved whether TdP onset in LQT3 is pause dependent or not. Of note, the quantitative effect of possible confounding by LQT3 is likely to be small, given the low prevalence of LQT3 (8% among genotyped LQTS patients and 5% of all LQTS patients[3]). In any case, these observations indicate that caution must be exercised when these studies and ours are interpreted because selection bias may result from the limited and disparate (between genotypes) availability of ECG documentation of TdP onset in congenital LQTS. Similarly, we cannot exclude that our findings apply mostly to severe LQTS patients who seek medical attention because of frequent TdP recurrences and that less severe cases may be underrepresented in this analysis.

Conclusion

Pause dependence of TdP onset is predominant in LQT2 but rare or absent in LQT1. This disparity may point to genotype-specific arrhythmia mechanisms and affect treatment strategies.

Disclosures

None.

References

1. Schwartz PJ, Moss AJ, Vincent GM, Crampton RS. Diagnostic criteria for the long QT syndrome: an update. *Circulation*. 1993;88:782–784.
2. Wilde AAM, Bezzina CR. Genetics of cardiac arrhythmias. *Heart*. 2005;91:1352–1358.
3. Splawski I, Shen J, Timothy KW, Lehmann MH, Priori S, Robinson JL, Moss AJ, Schwartz PJ, Towbin JA, Vincent GM, Keating MT. Spectrum of mutations in long-QT syndrome genes. *Circulation*. 2000;102:1178–1185.
4. Roden DM. Drug-induced prolongation of the QT interval. *N Engl J Med*. 2004;350:1013–1022.
5. Tan HL, Bezzina CR, Smits JPP, Verkerk AO, Wilde AAM. Genetic control of sodium channel function. *Cardiovasc Res*. 2003;57: 961–973.
6. Shimizu W. The long QT syndrome: therapeutic implications of a genetic diagnosis. *Cardiovasc Res*. 2005;67:347–356.
7. Moss AJ, Zareba W, Benhorin J, Locati EH, Hall WJ, Robinson JL, Schwartz PJ, Towbin JA, Vincent GM, Lehmann MH, Keating MT, MacCluer JW, Timothy KW. ECG T-wave patterns in genetically distinct forms of the hereditary long QT syndrome. *Circulation*. 1995; 92:2929–2934.
8. Wilde AAM, Jongbloed RJE, Doevendans PA, Düren DR, Hauer RNW, van Langen IM, van Tintelen JP, Smeets HJM, Meyer H, Geelen JLMC. Auditory stimuli as a trigger for arrhythmic events differentiate HERG-related (LQTS₂) patients from KVLQT1-related patients (LQTS₁). *J Am Coll Cardiol*. 1999;33:327–332.
9. Schwartz PJ, Priori SG, Spazzolini C, Moss AJ, Vincent GM, Napolitano C, Denjoy I, Guicheney P, Breithardt G, Keating MT, Towbin JA, Beggs AH, Brink P, Wilde AAM, Toivonen L, Zareba W, Robinson JL, Timothy KW, Corfield V, Wattanasirichaigoon D, Corbett C, Haverkamp W, Schulze-Bahr E, Lehmann MH, Schwartz K, Coumel P, Bloise R. Genotype–phenotype correlations in the long-QT syndrome: gene-specific triggers for life-threatening arrhythmias. *Circulation*. 2001;103:89–95.
10. van Langen IM, Birnie E, Alders M, Jongbloed RJ, Le Marec H, Wilde AA. The use of genotype–phenotype correlations in mutation analysis for the long QT syndrome. *J Med Genet*. 2003;40:141–145.
11. Zareba W, Moss AJ, Schwartz PJ, Vincent GM, Robinson JL, Priori SG, Benhorin J, Locati EH, Towbin JA, Keating MT, Lehmann MH, Hall WJ. Influence of the genotype on the clinical course of the long-QT syndrome. *N Engl J Med*. 1998;339:960–965.
12. Priori SG, Schwartz PJ, Napolitano C, Bloise R, Ronchetti E, Grillo M, Vicentini A, Spazzolini C, Nastoli J, Bottelli G, Folli R, Cappelletti D. Risk stratification in the long-QT syndrome. *N Engl J Med*. 2003;348:1866–1874.
13. Moss AJ, Zareba W, Hall WJ, Schwartz PJ, Crampton RS, Benhorin J, Vincent GM, Locati EH, Priori SG, Napolitano C, Medina A, Zhang

14. L, Robinson JL, Timothy KW, Towbin JA, Andrews ML. Effectiveness and limitations of β-blocker therapy in congenital long-QT syndrome. *Circulation*. 2000;101:616–623.
14. Priori SG, Napolitano C, Schwartz PJ, Grillo M, Bloise R, Ronchetti E, Moncalvo C, Tulipani C, Veia A, Bottelli G, Nastoli J. Association of long QT syndrome loci and cardiac events among patients treated with β-blockers. *JAMA*. 2004;292:1341–1344.
15. Noda T, Shimizu W, Satomi K, Suyama K, Kurita T, Aihara N, Kamakura S. Classification and mechanism of torsade de pointes initiation in patients with congenital long QT syndrome. *Eur Heart J*. 2004;25:2149–2154.
16. Locati EH, Zareba W, Moss AJ, Priori SG, Napolitano C, Benhorin J, Schwartz PJ. Torsades de pointes in patients with congenital long QT syndrome: spontaneous sequences of onset and offset from ECG recordings. *Pacing Clin Electrophysiol*. 1999;22:II-731. Abstract.
17. Moss AJ, Liu JE, Gottlieb S, Locati EH, Schwartz PJ, Robinson JL. Efficacy of permanent pacing in the management of high-risk patients with long QT syndrome. *Circulation*. 1991;84:1524–1529.
18. Viskin S. Cardiac pacing in the long QT syndrome: review of available data and practical recommendations. *J Cardiovasc Electrophysiol*. 2000;11:593–600.
19. Dorostkar PC, Eldar M, Belhassen B, Scheinman MM. Long-term follow-up of patients with the idiopathic long-QT syndrome treated with combined β-blockers and continuous pacing. *Circulation*. 1999; 100:2431–2436.
20. Tan HL, Hou CJY, Lauer MR, Sung RJ. Electrophysiologic mechanisms of the long QT interval syndromes and torsade de pointes. *Ann Intern Med*. 1995;122:701–714.
21. Viskin S, Fish R, Zeltser D, Belhassen B, Heller K, Brosh D, Laniado S, Barron HV. Arrhythmias in the congenital long QT syndrome: how often is torsade de pointes pause dependent? *Heart*. 2000;83:661–666.
22. Shimizu W, Ohe T, Kurita T, Takaki H, Aihara N, Kamakura S, Matsuhisa M, Shimomura K. Early afterdepolarizations induced by isoproterenol in patients with congenital long QT syndrome. *Circulation*. 1991;84:1915–1923.
23. Shimizu W, Antzelevitch C. Differential effects of beta-adrenergic agonists and antagonists in LQT1, LQT2 and LQT3 models of the long QT syndrome. *J Am Coll Cardiol*. 2000;35:778–786.
24. Viswanathan PC, Rudy Y. Pause induced early afterdepolarizations in the long QT syndrome: a simulation study. *Cardiovasc Res*. 1999;42: 530–542.
25. Marbán E, Robinson SW, Wier WG. Mechanisms of arrhythmogenic delayed and early afterdepolarizations in ferret ventricular muscle. *J Clin Invest*. 1986;78:1185–1192.
26. Burashnikov A, Antzelevitch C. Acceleration-induced action potential prolongation and early afterdepolarizations. *J Cardiovasc Electrophysiol*. 1998;9:934–948.
27. Burashnikov A, Antzelevitch C. Block of I_{Ks} does not induce early afterdepolarization activity but promotes β-adrenergic agonist-induced delayed afterdepolarization activity. *J Cardiovasc Electrophysiol*. 2000;11:458–465.
28. Liu J, Laurita KR. The mechanism of pause-induced torsade de pointes in long QT syndrome. *J Cardiovasc Electrophysiol*. 2005;16: 981–987.
29. Veldkamp MW, Verkerk AO, van Ginneken AC, Baartscheer A, Schumacher C, de Jonge N, de Bakker JM, Opthof T. Norepinephrine induces action potential prolongation and early afterdepolarizations in ventricular myocytes isolated from human end-stage failing hearts. *Eur Heart J*. 2001;22:955–963
30. Mazur A, Roden DM, Anderson ME. Systemic administration of calmodulin antagonist W-7 or protein kinase A inhibitor H-8 prevents torsade de pointes in rabbits. *Circulation*. 1999;100:2437–2442.
31. Terrenoire C, Clancy CE, Cormier JW, Sampson KJ, Kass RS. Autonomic control of cardiac action potentials: role of potassium channel kinetics in response to sympathetic stimulation. *Circ Res*. 2005;96:e25–e34.
32. Thomas D, Kiehn J, Katus HA, Karle CA. Adrenergic regulation of the rapid component of the delayed rectifier potassium current, I_{Kr}, and the underlying hERG ion channel. *Basic Res Cardiol*. 2004;99: 279–287.
33. Karle CA, Zitron E, Zhang W, Kathöfer S, Schoels W, Kiehn J. Rapid component I_{Kr} of the guinea-pig cardiac delayed rectifier K⁺ current is inhibited by β₁-adrenoceptor activation, via cAMP/protein kinase A-dependent pathways. *Cardiovasc Res*. 2002;53:355–362.

34. Zhang LM, Wang Z, Nattel S. Effects of sustained β-adrenergic stimulation on ionic currents of cultured adult guinea pig cardiomyocytes. *Am J Physiol.* 2002;282:H880–H889.

35. Heath BM, Terrar DA. Protein kinase C enhances the rapidly activating delayed rectifier potassium current, I_{Kr}, through a reduction in C-type inactivation in guinea-pig ventricular myocytes. *J Physiol.* 2000;522:391–402.

36. Viskin S, Alla SR, Barron HV, Heller K, Saxon L, Kitzis I, Hare GF, Wong MJ, Lesh MD, Sheinman MM. Mode of onset of torsade de pointes in congenital long QT syndrome. *J Am Coll Cardiol.* 1996; 28:1262–1268.

37. Tan HL, Alings M, van Olden RW, Wilde AAM. Long-term (subacute) potassium treatment in congenital HERG-related long QT syndrome (LQTS2). *J Cardiovasc Electrophysiol.* 1999;10:229–233.

CLINICAL PERSPECTIVE

The onset of torsade de pointes ventricular tachycardia in long-QT syndrome (LQTS) is generally believed to be pause dependent, being initiated by a short-long-short sequence of preceding RR intervals. We studied whether this initiating sequence is present in the 3 most common types of inherited LQTS (LQT1, LQT2, and LQT3). This analysis may provide insight into the mechanism of and rationale for treatment strategies in the various forms of LQTS, in particular, the use of β-adrenergic blockers and the ancillary use of pacemakers programmed with pause-preventing algorithms. Fifty genotyped LQT1, LQT2, and LQT3 patients were studied. Pause dependence was predominant in LQT2 but absent in LQT1. In LQT1, torsade de pointes started without significant changes in the duration of the preceding RR intervals. These findings point to different arrhythmia mechanisms and may explain why β-adrenergic blockers as single treatment are more effective in LQT1 than in LQT2. Ancillary treatment with pause-preventing pacemakers may be required in LQT2.

PRECLINICAL STUDIES

Cellular Basis for Trigger and Maintenance of Ventricular Fibrillation in the Brugada Syndrome Model
High-Resolution Optical Mapping Study

Takeshi Aiba, MD, PHD,* Wataru Shimizu, MD, PHD,† Ichiro Hidaka, MS,* Kazunori Uemura, MD,*
Takashi Noda, MD, PHD,* Can Zheng, PHD,* Atsunori Kamiya, MD,* Masashi Inagaki, MD,*
Masaru Sugimachi, MD, PHD,* Kenji Sunagawa, MD, PHD*

Suita, Japan

OBJECTIVES   We examined how repolarization and depolarization abnormalities contribute to the development of extrasystoles and subsequent ventricular fibrillation (VF) in a model of the Brugada syndrome.

BACKGROUND   Repolarization and depolarization abnormalities have been considered to be mechanisms of the coved-type ST-segment elevation (Brugada-electrocardiogram [ECG]) and development of VF in the Brugada syndrome.

METHODS   We used high-resolution (256 × 256) optical mapping techniques to study arterially perfused canine right ventricular wedges (n = 20) in baseline and in the Brugada-ECG produced by administration of terfenadine (5 μmol/l), pinacidil (2 μmol/l), and pilsicainide (5 μmol/l). We recorded spontaneous episodes of phase 2 re-entrant (P2R)-extrasystoles and subsequent self-terminating polymorphic ventricular tachycardia (PVT) or VF under the Brugada-ECG condition and analyzed the epicardial conduction velocity and action potential duration (APD) restitutions in each condition.

RESULTS   Forty-one episodes of spontaneous P2R-extrasystoles in the Brugada-ECG were successfully mapped in 9 of 10 preparations, and 33 of them were originated from the maximum gradient of repolarization (GR_{max}: 176 ± 54 ms/mm) area in the epicardium, leading to PVT (n = 12) or VF (n = 5). The epicardial GR_{max} was not different between PVT and VF. Wave-break during the first P2R-extrasystole produced multiple wavelets in all VF cases, whereas no wave-break or wave-break followed by wave collision and termination occurred in PVT cases. Moreover, conduction velocity restitution was shifted lower and APD restitution was more variable in VF cases than in PVT cases.

CONCLUSIONS   Steep repolarization gradient in the epicardium but not endocardium develops P2R-extrasystoles in the Brugada-ECG condition, which might degenerate into VF by further depolarization and repolarization abnormalities.   (J Am Coll Cardiol 2006;47:2074–85) © 2006 by the American College of Cardiology Foundation

Brugada syndrome is characterized by ST-segment elevation in the right precordial leads (V_1 to V_3) of electrocardiography (ECG) and a high incidence of ventricular fibrillation (VF) leading to sudden cardiac death (1–4). However, not all of the patients with ST-segment elevation have arrhythmic events (5,6), indicating that additional

factors might contribute to development of VF. Previous studies suggest that an accentuation of transient outward potassium current (I_{to})-mediated phase 1 notch and loss of action potential (AP) dome in some areas of the right ventricular (RV) epicardium but not endocardium increases transmural dispersion of repolarization (DR), which causes the ST-segment elevation (7–11). The heterogeneous loss of AP dome in the epicardium also increases epicardial DR, and a propagation of AP dome from a site where AP dome is restored to a site where it is lost might develop a local re-excitation called a phase 2 re-entry (P2R), which triggers a circus movement re-entry in the form of VF (8,9,12). It is still unclear, however, to what extent the epicardial DR is required for development of P2R and how phase 2 re-entrant (P2R)-extrasystoles produce VF. Moreover, depolarization abnormality is thought to be one of the potent arrhythmic substrate in the Brugada syndrome (13–17), but it is not fully understood how depolarization and repolar-

Abbreviations and Acronyms

AP	= action potential
APD	= action potential duration
APD_{50}	= action potential duration measured at 50% repolarization
BCL	= basic cycle length
Brugada-ECG	= coved-type ST-segment elevation
Delta-Epi interval	= interval from the earliest to the latest epicardial activation
DR	= dispersion of repolarization
ECG	= electrocardiogram/electrocardiography
GR_{max}	= maximum gradient of repolarization
I_{Ca}	= inward calcium current
I_{K-ATP}	= ATP-sensitive potassium current
I_{Na}	= sodium current
I_{to}	= transient outward potassium current
P2R	= phase 2 re-entrant/entry
RV	= right ventricle/ventricular
Sti-Epi interval	= interval from the stimulus to the earliest epicardial activation
VF	= ventricular fibrillation
VT	= ventricular tachycardia

ization abnormalities interact and contribute to the development and maintenance of VF in the Brugada syndrome.

To investigate the heterogeneities of cellular repolarization and depolarization and their potential role in the development of re-entrant arrhythmias, we used a technique of high-resolution optical mapping, which allowed us to measure the electrical heterogeneity of APs on the epicardial or endocardial surface (18). We demonstrated that a steep repolarization gradient in the RV epicardium but not in the endocardium plays a key role in initiating P2R. Moreover, further depolarization and repolarization abnormalities degenerate the P2R-induced spiral re-entry into multiple wavelets forming VF in an experimental model of the Brugada syndrome.

METHODS

Canine RV wedge model of the Brugada syndrome. All animal care procedures were in accordance with the position of the American Heart Association research animal use (November 11, 1984). The methods used for isolation, perfusion, and recording of transmembrane activity from the arterially perfused canine RV (anterior wall) is similar to methods reported with canine wedge preparations (8,9). Briefly, a transmural wedge with dimensions of approximately $2 \times 1 \times 0.7$ cm to $3 \times 1.5 \times 1$ cm was dissected from the free wall of the RV of male dogs (n = 20), cannulated via the branch of right coronary artery, and placed in a small tissue bath. These preparations were arterially perfused between 40 and 60 mm Hg with Tyrode's solution ($35 \pm 1°C$). The inward calcium current (I_{Ca}) and sodium current (I_{Na}) block with terfenadine (5 μmol/l), combined with augmentation of ATP-sensitive potassium current (I_{K-ATP}) with pinacidil (2 μmol/l), and I_{Na} block

with pilsicainide (5 μmol/l) were used to create an experimental model of the Brugada syndrome (8–10,19).

After changing ECG to the coved-type ST-segment elevation mimicking the Brugada syndrome (Brugada-ECG) by administration of these drugs, 1) we recorded the spontaneous occurrence of closely coupled extrasystoles and subsequent non-sustained polymorphic VT (terminated within 5 s) or VF (sustained more than 5 s) during pacing from the endocardium at basic cycle length (BCL) of 2,000 ms (n = 10), and 2) we analyzed restitutions of the epicardial conduction velocity and action potential variable with a single extra stimulus (S2) delivered after every 10th basic beat (S1) paced from the epicardial surface at BCL of 1,000 ms (n = 10).

Transmembrane AP and ECG recording. A transmural ECG was recorded with Ag-AgCl electrodes, which were placed in the Tyrode's solution bathing the preparation, 1.0 cm from the epicardial and endocardial surfaces (epicardial, positive pole). The epicardial and endocardial APs were simultaneously recorded from the epicardial and endocardial surfaces with separate intracellular floating microelectrodes (direct current resistance 10 to 20 MΩ; 2.7 mmol/l potassium chloride) at positions approximating the transmural axis of the ECG.

Optical AP recording. After staining with the voltage sensitive dye, di-4-ANEPPS (5 μmol/l for 30 min), wedges were stabilized against a flat imaging window. Excitation of the dye's fluorescence was achieved with 480 ± 15 nm light through a bandpass filter (ANDV8247, Andover, Salem, New Hampshire) from a bluish-green emission diode (E1L51-3B0A4-02, Toyoda Gosei, Aichi, Japan). Fluoresced light from the wedge was split by a dichrotic mirror and narrowed down to the two frequency bands (approximately 540 or 690 nm) through a bandpass filter (ANDV8368 or ANDV7845, respectively, Andover). Then, the dual-wavelength lights were simultaneously focused onto 10-bit 256 × 256 element dual complementary metal oxide semiconductor (C-MOS) censors (Hamamatsu Photonics, Hamamatsu, Japan) with image intensifiers (FASTCAM-Ultima, Photron, Tokyo, Japan) at a 500 frames/s (Fig. 1).

Both optical signals were digitized at 0.5 kHz, and other amplified signals were digitized at 2 kHz with a 12-bit analog-to-digital converter, stored on the hard disk of a dedicated laboratory computer system, and analyzed with the original software of our laboratory. Therefore, after ratiometry of both signals to subtract a motion artifact, the voltage of the optical signal recorded at each site was automatically displayed in color (lowest, black; greatest, red) and plotted in the 256 × 256 matrix as an isopotential map, and transmembrane APs from 256 sites (16 × 16 units) on the RV epicardial or endocardial surface were displayed in control and in the Brugada-ECG condition with or without arrhythmic events. Moreover, phase analysis was used to display the pattern of wave propagation and wave-break during ventricular tachyarrhythmias (20,21).

Data analysis. Optical action potential duration (APD) was automatically measured at 50% repolarization (APD_{50}),
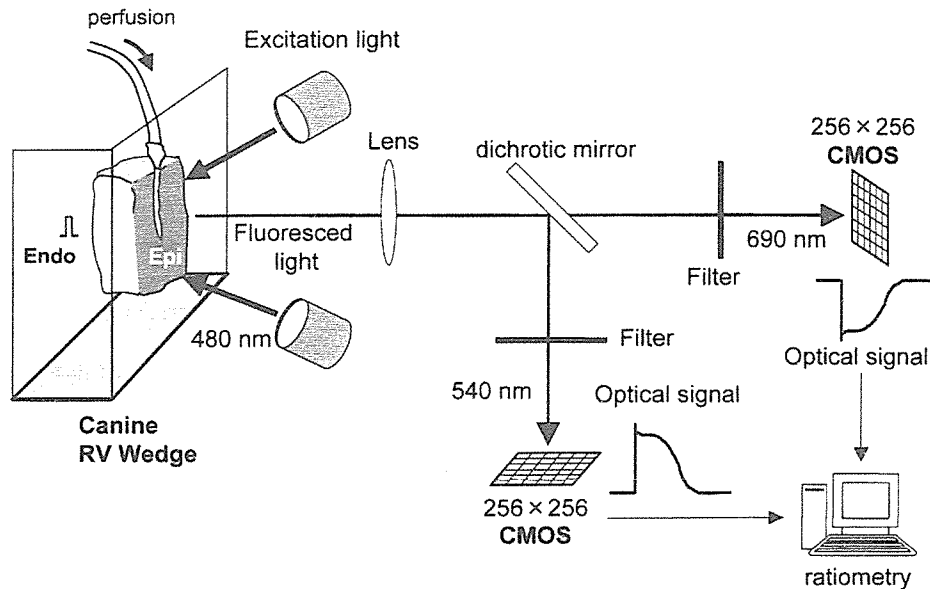
Figure 1. Schematic diagram showing the major components of high-resolution optical mapping of the epicardial (Epi) or endocardial (Endo) surface in an arterially perfused canine right ventricular (RV) wedge preparation. CMOS = complementary metal oxide semiconductor.

and the distributions of epicardial and endocardial APD_{50} were displayed as a repolarization counter map in baseline (control condition) and after changing to the Brugada-ECG with or without P2R-extrasystoles. The epicardial and endocardial DR were calculated from the maximum difference of repolarization times (activation time + APD) in the epicardial and endocardial surfaces, respectively. Transmural DR was calculated from the maximum difference between the epicardial and endocardial repolarization times recorded from the floating microelectrodes. Moreover, the maximum gradient of repolarization (GR_{max} = maximum Delta-APD_{50}/Delta-distance) in the epicardium and endocardium were calculated in each condition. We also measured depolarization parameters such as the interval from the stimulus to the earliest epicardial activation (Sti-Epi interval) and the interval from the earliest to the latest epicardial activation (Delta-Epi interval) during pacing from the endocardium in control and in the Brugada-ECG
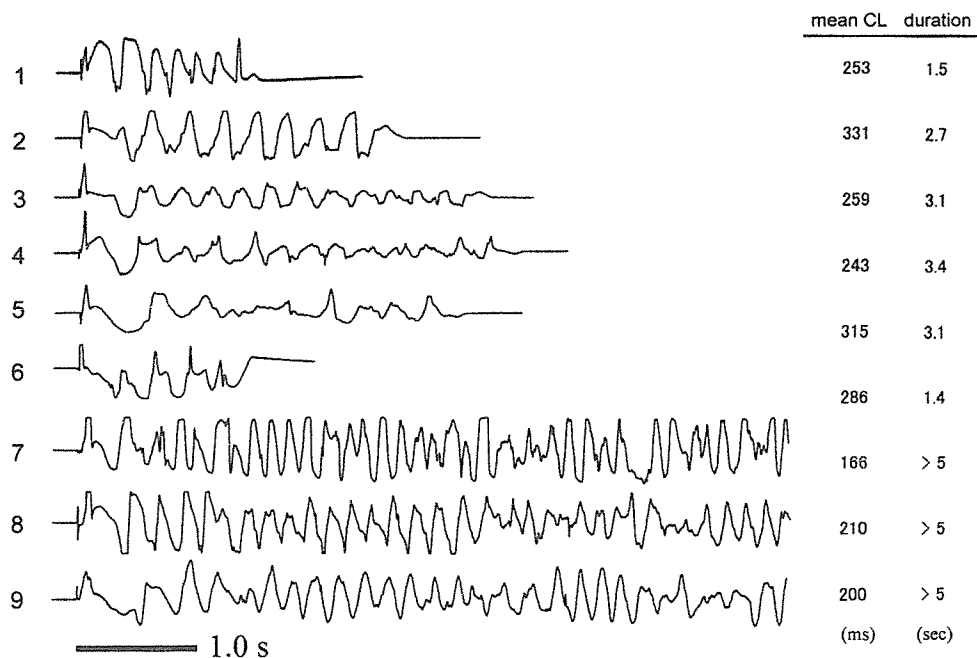

	mean CL	duration
1	253	1.5
2	331	2.7
3	259	3.1
4	243	3.4
5	315	3.1
6	286	1.4
7	166	> 5
8	210	> 5
9	200	> 5
	(ms)	(sec)

1.0 s

Figure 2. Representative episodes of polymorphic ventricular tachycardia or ventricular fibrillation (VF) in a canine wedge model of the Brugada syndrome. All arrhythmias were spontaneously developed after the electrocardiogram with coved-type ST-segment elevation. Many of the arrhythmias (numbers 1 to 6) terminated within a few seconds, but the others (numbers 7 to 9) with a shorter cycle length (CL) degenerated into VF, which continued more than 5 s.

condition. Conduction velocity (θ) was determined by linear regression of the isochrone distance versus activation time. Lines parallel and perpendicular to the fiber orientation were defined as the direction of longitudinal (L) and transverse (T) propagation, respectively. The optical data at edge of the preparation, with apparent contraction artifact, and noise level more than 20% of AP amplitude were excluded.

Statistical analysis. Statistical analysis of the data was performed with a Student's t test for paired data or analysis of variance coupled with Scheffe's test, as appropriate. Data is expressed as mean ± SD or mean ± SEM. Significance was defined as a value of $p < 0.05$.

RESULTS

Canine wedge model of the Brugada syndrome. Terfenadine combined with pinacidil and pilsicainide produced the Brugada-ECG in all preparations. There was no arrhythmia in control conditions, whereas combination of the drugs spontaneously developed a P2R-induced short-coupled extrasystole and subsequent polymorphic VT or VF in 9 of 10 preparations (Fig. 2). The QRS interval, QT interval, and J-point level in the ECG were significantly greater in the Brugada-ECG than in the control condition, but those parameters in the Brugada-ECG were not significantly different between beats with and without P2R-extrasystoles (Table 1).

Epicardial repolarization abnormality develops P2R-extrasystoles. Figure 3 represents the epicardial and endocardial APD_{50} contour map and optical APs in the control and in the Brugada-ECG condition with or without P2R-extrasystoles. In the control condition, the epicardial and endocardial APs were almost homogeneous (Figs. 3A and 3D). In contrast, in the Brugada-ECG, the AP morphology in the epicardium but not endocardium changed into heterogeneous, owing to a combination of abbreviated (loss-of-dome) and prolonged (restore-of-dome) APs, resulting in increasing DR in the epicardium rather than in the endocardium (Figs. 3B and 3E). Moreover, further prolonged AP at some areas in the epicardium was closely adjacent to the loss-of-dome APs (arrow), thus producing a repolarization mismatch within a small area and developing a P2R-extrasystole at the loss-of-dome site (Fig. 3C). The APs in the endocardium, however, were less heterogeneous than those in the epicardium even in the Brugada-ECG just before P2R-extrasystoles (Fig. 3F).

The composite data of repolarization and depolarization parameters in the control and in the Brugada-ECG condition with and without P2R-extrasystoles are shown in Table 1. In the Brugada-ECG, the epicardial maximum APD_{50} was significantly prolonged, whereas the epicardial minimum APD_{50} was significantly abbreviated compared with those in the control condition, thus significantly increasing the epicardial DR and GR_{max}. Moreover, the

Table 1. ECG, Repolarization, and Depolarization Parameters in Control and in the Brugada-ECG Condition With or Without Phase 2 Re-Entrant Extrasystoles

		Brugada-ECG	
	Control	P2R-PVC (−)	P2R-PVC (+)
ECG			
QRS duration (ms)	35 ± 4	63 ± 20*	66 ± 22*
QT interval (ms)	286 ± 30	335 ± 33*	—
J-point (mV)	0.04 ± 0.04	0.23 ± 0.08*	0.27 ± 0.08*
Repolarization			
Epicardium			
Max APD_{50} (ms)	239 ± 19	325 ± 86*	480 ± 92*†
Min APD_{50} (ms)	192 ± 16	100 ± 32*	89 ± 28*
Mean APD_{50} (ms)	214 ± 18	200 ± 62	244 ± 68†
DR (ms)	47 ± 11	228 ± 78*	383 ± 93*†
GR_{max} (ms/mm)	5 ± 5	46 ± 29*	176 ± 54*†
Endocardium			
Max APD_{50} (ms)	269 ± 23	269 ± 61	314 ± 77
Min APD_{50} (ms)	214 ± 28	171 ± 53	183 ± 55
Mean APD_{50} (ms)	244 ± 27	219 ± 63	258 ± 70
DR (ms)	56 ± 13	98 ± 44	123 ± 41*
GR_{max} (ms/mm)	8 ± 4	20 ± 13	26 ± 10*
Transmural			
DR (ms)	28 ± 8	135 ± 36*	131 ± 41*
Depolarization			
Sti-Epi interval (ms)	26 ± 10	46 ± 9*	47 ± 12*
Delta-Epi interval (ms)	12 ± 4	19 ± 18	24 ± 20

Values are mean ± SD. *$p < 0.05$ versus control; †$p < 0.05$ versus coved-type ST-segment elevation (Brugada-ECG) condition without P2R-PVC by analysis of variance with Scheffe's test.

APD_{50} = action potential duration at 50% repolarization; Delta-Epi = interval from the earliest to the latest epicardial activation; DR = dispersion of repolarization; GR_{max} = maximum gradient of repolarization; Max = maximum; Min = minimum; P2R-PVC = phase 2 re-entrant extrasystoles; Sti-Epi = interval from the stimulus to the epicardium.
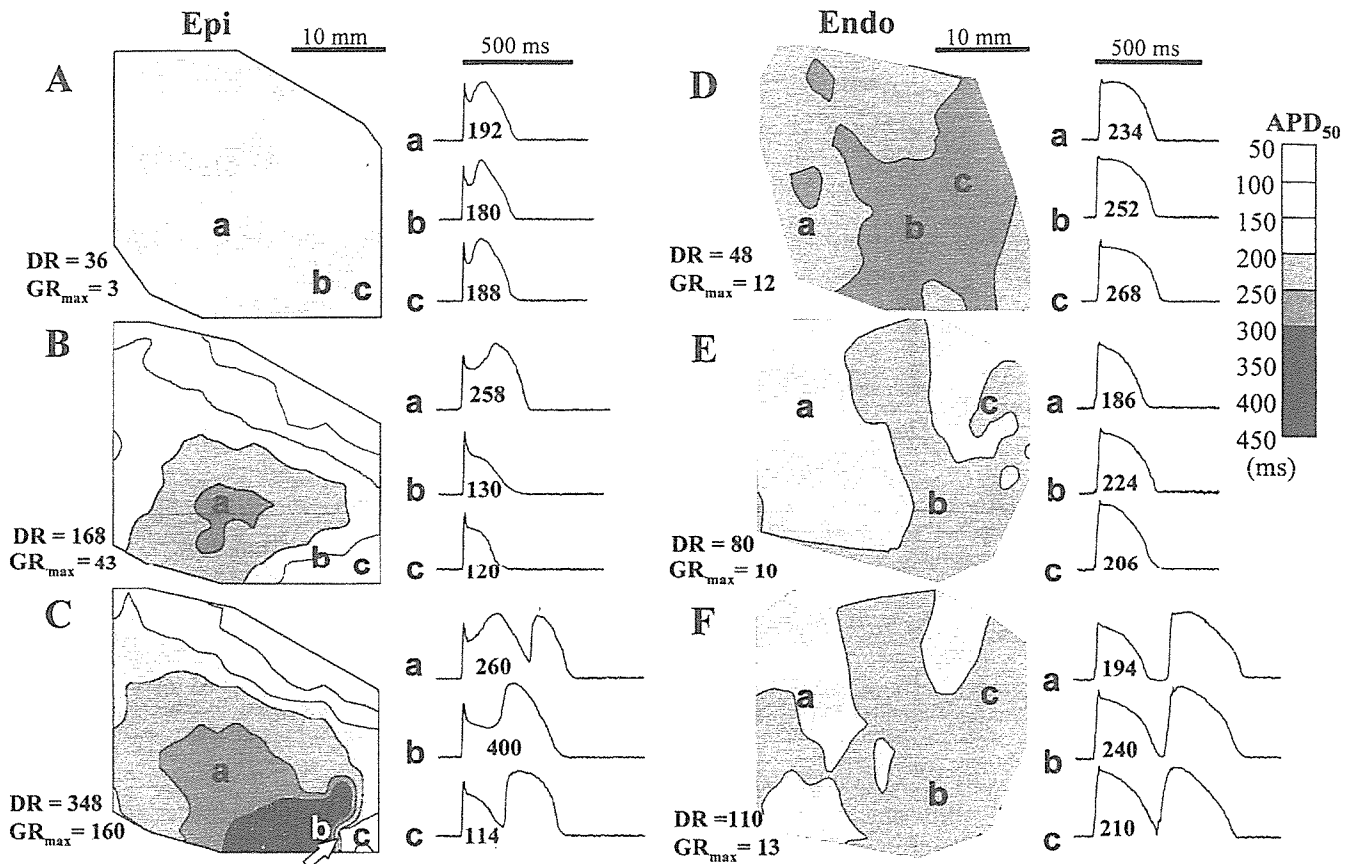
Figure 3. Representative action potential duration measured at 50% repolarization (APD_{50}) contour map on the right ventricular epicardium (Epi) and endocardium (Endo) in control condition (**A and D**, respectively), in the ST-segment elevation (Brugada-ECG) without phase 2 re-entrant (P2R) extrasystoles (**B and E**, respectively), and in the Brugada-ECG just before P2R extrasystoles (**C and F**, respectively) and representative optical action potentials at each site (**a to c**). **White arrow** = initial site of P2R. DR = dispersion of repolarization; GR_{max} = maximum gradient of repolarization.

epicardial maximum APD_{50} was further prolonged in the Brugada-ECG just before P2R-extrasystoles compared with that without P2R-extrasystoles, thus remarkably increasing the epicardial DR and GR_{max}. The endocardial repolarization parameters, however, were not significantly changed after the Brugada-ECG. Moreover, there was no significant difference in the endocardial repolarization parameters between the Brugada-ECG with and without P2R-extrasystoles. Owing to a different response of APD between the epicardium and endocardium, transmural DR was significantly increased in the Brugada-ECG compared with that in the control condition but was not significantly different between the Brugada-ECG condition with and without P2R-extrasystoles.

Regarding depolarization parameters, the Sti-Epi interval was significantly increased in the Brugada-ECG compared with in the control condition but was not different between the condition with and without P2R-extrasystoles. The Delta-Epi interval was not significantly different among the three conditions.

Threshold to develop P2R-extrasystoles. A total of 41 episodes of spontaneous P2R-extrasystoles after the Brugada-ECG were successfully mapped in 9 of 10 preparations, and 33 (80%) of them were originated from the

GR_{max} area in the epicardium. As shown in Figure 4, the epicardial GR_{max} was significantly greater in the Brugada-ECG than in control condition. The GR_{max} of 99 ms/mm (dashed line) showed that P2R-extrasystoles were spontaneously developed in the Brugada-ECG. In contrast, the endocardial GR_{max} and transmural DR were greater in the Brugada-ECG condition compared with the control condition but were not different between the Brugada-ECG condition with and without P2R-extrasystoles.

Figure 5A shows the epicardial isopotential map representing the distribution of loss-of-dome and restore-of-dome area in the Brugada-ECG with (beat 2) or without (beat 1) a P2R-extrasystole. Figures 5B and 5C show the depolarization map during the P2R-extrasystole and optical APs at each site on the epicardial surface. At the timing of phase 2 (120 to 190 ms), the restore-of-dome area (orange-red) was larger in the beat 2 than in the beat 1. Moreover, the larger AP dome in the beat 2 moved from a restore-of-dome site (site a and b) to a nearby loss-of-dome site (site d), producing re-excitation at the loss-of-dome site and propagating in a counterclockwise fashion around the refractory region of the epicardium.

P2R-extrasystoles induce polymorphic VT or VF. The epicardial P2R-extrasystoles produced 12 episodes of self-
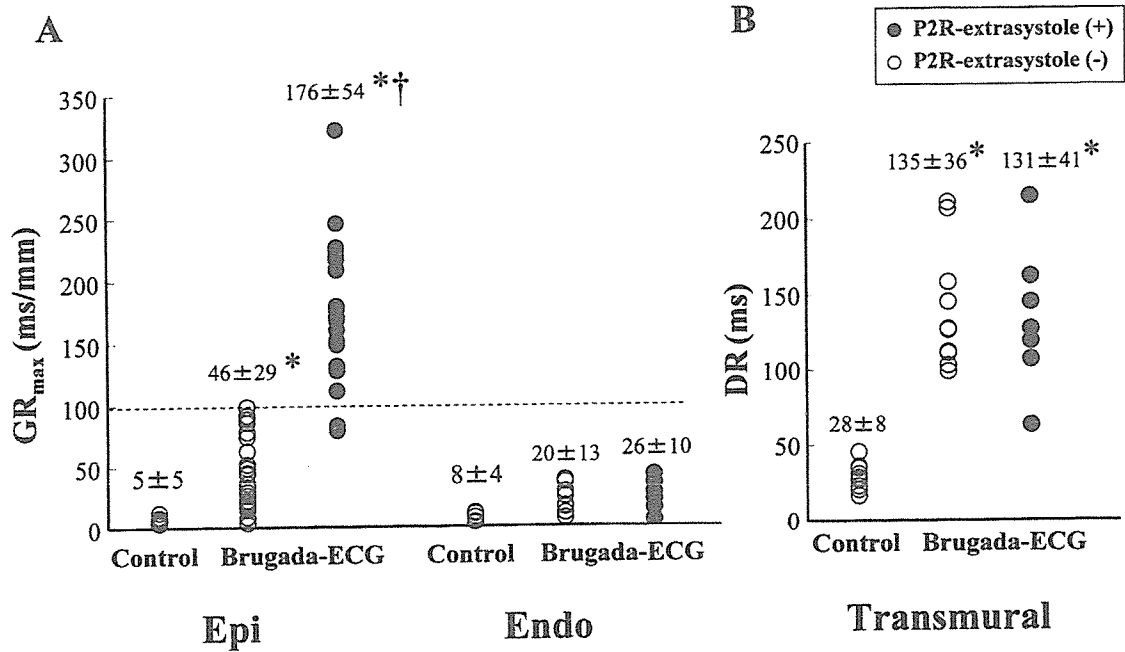
Figure 4. Scatter plots of the maximum gradient of repolarization (GR_{max}) in the epicardial (Epi) and endocardial (Endo) surfaces (**A**) and transmural dispersion of repolarization (DR) (**B**) in control and the ST-segment elevation (Brugada-ECG) condition with (**closed circles**) or without (**open circles**) phase 2 re-entrant (P2R) extrasystoles. Values are mean ± SD. *p < 0.05 versus control condition; †p < 0.05 versus Brugada-ECG condition without P2R-extrasystole by analysis of variance with Scheffe's test.

terminating (<5 s) polymorphic VT and 5 episodes of sustained (≥5 s) VF. The mechanism underlying the difference between the polymorphic VT and VF is shown in representative examples in Figures 6 and 7. The epicardial GR_{max} area (arrow) developed P2R-extrasystole in both cases (Figs. 6A and 7A); however, the epicardial depolarization map paced from the endocardium at BCL of 2,000 ms shows a remarkable conduction delay in the episode of VF (Fig. 7B) compared with that of polymorphic VT (Fig. 6B). We compared the repolarization and depolarization parameters just before the P2R-induced polymorphic VT and VF in Table 2. There was no significant difference in the repolarization parameters between the two groups; however, the depolarization parameters such as QRS, Sti-Epi, and Delta-Epi intervals were significantly longer in the VF group than in the polymorphic VT group.

Figures 6C and 6D represent phase map and optical APs, respectively, during the P2R-induced polymorphic VT, showing that re-entry was initiated from the epicardial GR_{max} area and rotated mainly in the epicardium without wave-break. In contrast, Figures 7C and 7D represent those during the P2R-induced VF, showing that the development of initial P2R was similar to that of polymorphic VT, but the first P2R-wave was broken up into the multiple wavelets, resulting in degenerating VT into VF. The phase singularity points during the first P2R-wave almost coincided with the sites of delayed conduction (Fig. 7B). In all VF cases, the wave was broken up into multiple wandering wavelets during the first P2R-induced extrasystole; however, in the polymorphic VT cases, only 3 of 12 (25%) cases had a wave-break after the second beat, but soon

after the wave had been broken, the waves collided and finally terminated.

Conduction and APD restitutions by S1-S2 method. In another 10 preparations, we analyzed the epicardial conduction velocity and APD restitutions to show the mechanisms underlying the wave-break during the first re-entrant wave in the VF cases. The epicardial longitudinal and transverse conduction velocities (θ_L and θ_T) in the VF cases (n = 5) were significantly slower than those in the polymorphic VT cases (n = 5) under the Brugada-ECG condition, and the conduction velocity restitution curve in the VF cases was shifted lower in parallel (Fig. 8).

In contrast, the epicardial APD was abbreviated and its restitution was flat in the polymorphic VT case under the Brugada-ECG condition, owing to loss of AP dome (Fig. 9B); however, in the VF case, shorter S1-S2 interval (≤300 ms) rather prolonged APD because of restoration of AP dome. Moreover, this restoration was heterogeneous in the epicardial surface, increasing the epicardial DR (Fig. 9C). This "inverse" APD restitution pattern was observed in four of five VF cases but in only one of five polymorphic VT cases under the Brugada-ECG condition.

DISCUSSION

Repolarization mismatch develops P2R-extrasystoles. All-or-none repolarization of the ventricular AP and P2R is considered to be one of the potential mechanism of the ST-segment elevation and subsequent VF in the Brugada
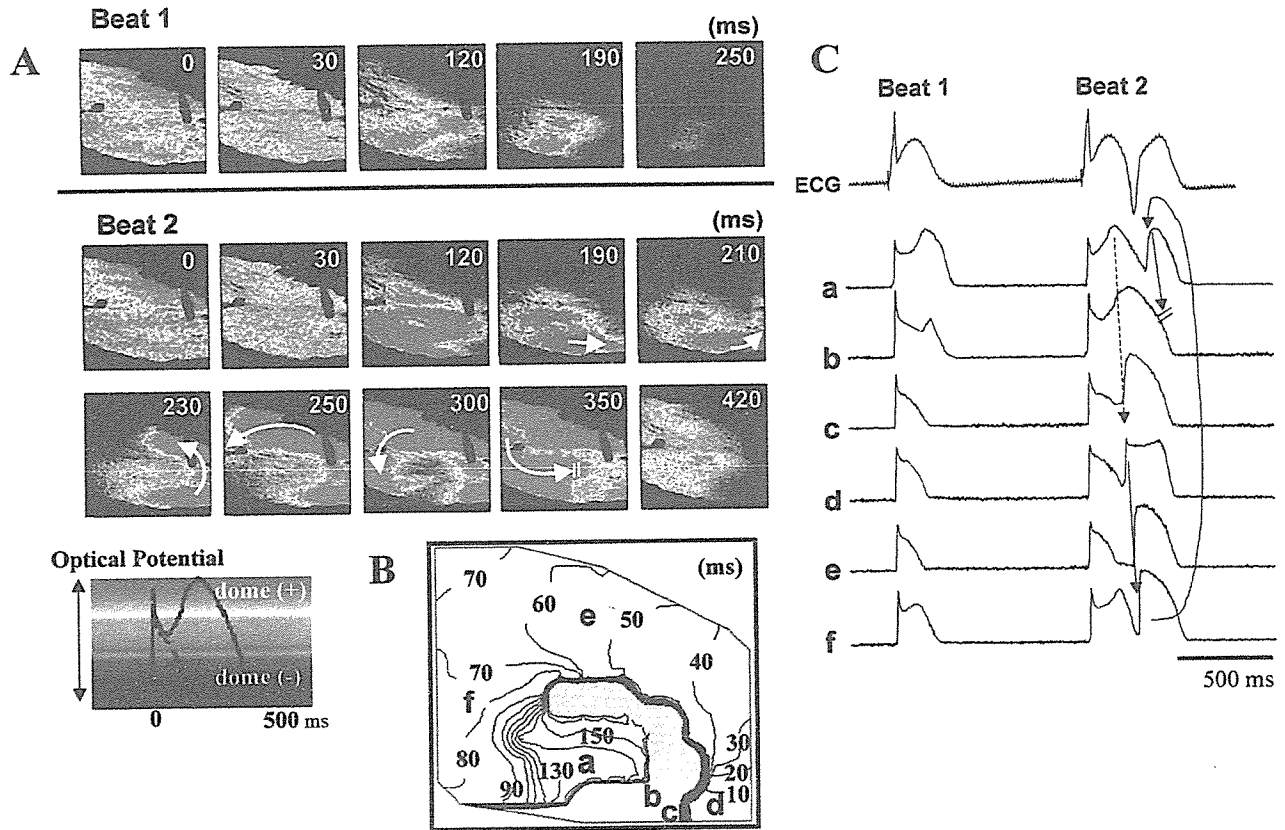
Figure 5. Snapshots of a color optical isopotential movie on the epicardial surface for the continuous two beats with (Beat 2) and without (Beat 1) a phase 2 re-entrant extrasystole (P2R-extrasystole) in the Brugada-ECG condition (A). Depolarization map of a P2R-extrasystole (B) and optical action potentials at each site (a to f) and transmural electrocardiogram (ECG) (C). Please see the Appendix for accompanying video.

syndrome (7–9,12); however, because of limitations of conventional electrophysiological recording techniques, it remains unknown to what extent the heterogeneity of APs is required for developing P2R-extrasystoles in the Brugada-ECG. In this study, we conducted a high-resolution optical mapping in canine RV wedge preparation, which allowed a detailed measurement of cellular repolarization and depolarization in the epicardial and endocardial surfaces. First, we photographed the moment that P2R-extrasystoles in the Brugada-ECG occurred and produced re-entrant arrhythmias such as polymorphic VT or VF. A unique topographical distribution of both loss-of-dome and restore-of-dome cells in the epicardium but not endocardium might underlie a key feature of the Brugada phenotype, including coved-type ST-segment elevation and susceptibility to P2R-induced ventricular tachyarrhythmias. It must be essential to develop P2R-extrasystoles that further prolong the epicardial AP results in loss-of-dome at some areas but not at the closely adjacent area, making a steep repolarization mismatch. These data are consistent with some clinical reports that the QT interval is more prolonged in the right precordial leads than in other leads during typical coved-type Brugada-ECG (2,13,22) and that VF in the Brugada syndrome was frequently induced by the specific

premature ventricular contractions originated from the free wall of RV outflow tract (23,24).

Ionic backgrounds of Brugada-ECG and P2R-extrasystoles. Previous experimental studies pharmacologically created the Brugada-ECG by using various drugs and/or conditions capable of causing an outward shift in the current active at the end of phase 1 of RV epicardium (e.g., increase in I_{to}, I_{K-ATP}, and/or I_{K-ACh} and decrease in I_{Ca} and I_{Na}) (4,7–10,19). Moreover, a development of P2R on the basis of the all-or-none repolarization phenomenon might depend on a fine balance of I_{to}, I_{Na}, and I_{Ca}. We used block of I_{Ca} and I_{Na} (and other currents) with terfenadine (5 µmol/l), combined with augmentation of I_{K-ATP} with pinacidil (2 µmol/l) and I_{Na} block with pilsicainide (5 µmol/l); a combination that is most likely to produce the Brugada-ECG. The reason a loss-of-dome occurred in some areas but not others in the epicardium is expected to be owing to an intrinsic difference in I_{to} (25). Miyoshi et al. (26) investigated the mechanism of P2R by their mathematical model and suggested that P2R was developed from a boundary area (0.8 cm) between loss-of-dome and restore-of-dome where a fine balance between I_{to} and $I_{Ca,L}$ was required and that $I_{Ca,L}$ must play an essential role in the genesis of P2R. This mathematical model